November 2014

Modification of Gold Nanoparticles for SERS Application in Emulsion and Lipid Systems

Michael J. Driver
University of Massachusetts Amherst

Modification of Gold Nanoparticles for SERS Application in Emulsion and Lipid Systems

A Thesis Presented

By

MICHAEL J. DRIVER

Submitted to the Graduate School of the
University of Massachusetts Amherst in partial fulfillment
of the requirements for the degree of

Master of Science

September 2014

Department of Food Science

Modification of Gold Nanoparticles for SERS Application in Emulsion and Lipid Systems

A Thesis Presented

By

MICHAEL J. DRIVER

Approved as to style and content by:

_____
Lili He, Chair

_____
Eric Decker, Member

_____
Guodong Zhang, Member

_____
Eric Decker, Department Head
Food Science

ACKNOWLEDGMENTS

I would like to thank my advisor Dr. Lili He for her full support and encouragement throughout my research. The experience I gained and opportunities I had in this lab greatly exceeded my expectations, for which I am grateful. I would also like to thank Dr. Decker and Dr. Zhang for being members on my committee and for their input on my thesis. I would finally like to thank Dr. McClements for his input and assistance throughout my project.

Aside from the professors, I would like to acknowledge and thank my lab mates, for their help and support over the years as well as lab members from throughout the department where their expertise was greatly appreciated.

ABSTRACT

MODIFICATION OF GOLD NANOPARTICLES FOR SERS APPLICATION IN EMILSION AND LIPID SYSTEMS

SEPTEMBER 2014

MICHAEL J. DRIVER, B.S., RUTGERS UNIVERSITY

M.S., UNIVERSITY OF MASSACHUSETTS AMHERST

Directed by: Professor Lili He

Gold nanoparticles produced using the Turkevich method were able to have their hydrophobicity modified using octanethiol in a novel method for SERS application. Both amphiliphic GNPs and hydrophobic GNPs were produced and differentiated by Raman signals. The amphiliphic GNPs were able to enhance the SERS signals of the protein emulsifier in the emulsion *in situ* and the hydrophobic GNPs were able to enhance the SERS signals from canola oil. Further purification of the hydrophobic GNPs proved to have higher enhancement and sensitivity, but still poor consistency which is typical of SERS. Monitoring lipid oxidation using Raman and SERS using alternative approaches was the primary objective of the thesis. The purified GNPs were capable of enhancing the canola oil over two weeks, but the poor consistency led to no major trends. Using normal Raman, a triphenylphosphine oxidation reaction was capable of producing a peroxide value correlation in a very simple and rapid manor. Using a gold nanoparticle modified stainless steel wire, the headspace volatiles from canola oil oxidation were able to be enhanced, but with poor consistency. Silver dendrites were used to enhance the canola oil signal but with poor resolution. A combination of silver dendrites and GNPs were used to slightly improve enhancement, but not as strong as GNPs alone.

TABLE OF CONTENTS

Page

LIST OF TABLES

Page

LIST OF FIGURES

Page

LIST OF ABBREVIATIONS

GNP – Gold Nanoparticles
SERS – Surface-enhanced Raman Spectroscopy

CHAPTER 1

INTRODUCTION

Raman spectroscopy is a vibrational spectroscopy which is capable of providing a fingerprint spectrum of a compound based on its molecular structure. It measures the amount of light that is scattered inelastically, which only accounts for 1 in 10,000,000 photons. The rest of the photons are scattered elastically, called Rayleigh scattering. Although Raman scattering is relatively weak, advances in laser and receptor technology have made Raman spectroscopy a very useful tool for sample characterization and identification. It is commonly used for quality control in the pharmaceutical industry to identify and validate ingredients. It is also used in threat detection, determining different types of explosives.(McCreery, 2000) Applying Raman spectroscopy to food samples is not new either, although industrial-wide it is not as popular as infrared spectroscopy. There are several reports on using Raman spectroscopy to measure edible oils. For example, there was a study performed to characterize 21 different types of food lipids which demonstrated that it is possible to discriminate between different types of similar oils using Raman spectroscopy (Baeten & Hourant, 1998). Another study was done to discriminate hazelnut oil contamination in olive oil, which is a practical analytical issue in the olive oil industry involving longer and more complicated methods (Baeten et al., 2005). In addition, two Raman characterization studies were done to monitor the oxidation process of oil (Muik, Lendl, Molina-Díaz, & Ayora-Cañada, 2005; Muik, Lendl, Molina-Diaz, Valcarcel, & Ayora-Cañada, 2007).

However, since Raman scattering is relatively weak, it has not been considered a sensitive measurement for lipid oxidation, especially compared to traditional techniques. Recently, a new technique called Surface Enhanced Raman Spectroscopy (SERS) is able to enhance Raman signals significantly, making Raman measurements much more sensitive. SERS utilizes noble metal nanostructures, such as gold or silver nanoparticles, to enhance the Raman scattering of a sample through a phenomenon called localized surface plasmon resonance. However, the sample must be within only a few nanometers of the nanoparticles in order to be enhanced (Zheng & He, 2014).

Gold nanoparticles (GNPs) are colloidal and less susceptible to oxidation which makes them a better substrate for this application. There are two major sample preparations for SERS samples: the substrate method in which the GNPs are placed on a slide and dried then the sample placed on top; or the solution method where the GNPs are mixed with the sample, and the mixture is placed on the slide. Previously, we used the substrate method for testing lipid oxidation on silver dendrites, but the sensitivity was not very satisfactory. The solution method is a preferable way because it allows the GNPs to bind with the sample molecules more uniformly. However, as most of the GNPs are prepared in aqueous conditions, they are not compatible with the oil. Therefore, the GNPs must be modified. Thiol containing compounds have been used to modify the surface chemistry of the GNPs due to their strong binding affinity to gold (Weisbecker, Merritt, & Whitesides, 1996). The objective of our study is to modify the hydrophobicity of the GNPs using octanethiol. The modified GNPs will be used to measure lipid oxidation products, and compare them with the traditional methods for measuring lipid oxidation.

In our novel method of modification, we mixed gold nanoparticles, octanethiol, and isopropyl alcohol for three days, allowing the thiols to fully bind to the gold surface. Isopropyl alcohol was used because it has a polarity in between that of water and hexane, and similar to that of octanethiol so it can be evenly distributed among the GNPs. After mixing, hexane was added as the final solvent. To concentrate the GNPs, we only used a quarter of the hexane as the original colloidal GNP mixture, effectively concentrating the gold 4×. When the hexane was added, the nanoparticles immediately accumulated at the interface of the aqueous-alcohol mixture and hexane. A brief three minute homogenization helped push the nanoparticles up into the hexane for extraction. Purification of the hydrophobic GNPs was performed to purge the solution of excess octanethiol, which had the potential to mask SERS signals. The GNPs were evaporated and hexane was added, in a cycle done three times.

Alternative tests were also tested for more specific compounds. A normal Raman test of TPP was also performed as a more consistent test, without SERS. The method was altered from an infrared spectroscopy method for application with Raman (Ma, Voort, Ismail, Zhuo, & Cheng, 2000). TPP is converted into TPPO by presence of hydrogen peroxides and can be measured by Raman. Next, the volatiles can be captured by a gold modified stainless steel wire (Feng et al., 2010). These wires can then be tested by Raman for volatile compounds produces by lipid oxidation.

Oil enhancement was also tested using silver dendrites, as a simple substrate method. Additionally, the sandwich method was tested which incorporated the GNP solution method, then placed on top of silver dendrites (J. Yang, Tan, Shih, & Cheng,

2014). The combination of two SERS substrates has the potential to be stronger than an individual substrate.

CHAPTER 2

LITERATURE REVIEW

2.1. Raman spectroscopy

2.1.1. History

Inelastic light scattering was first technically proposed in 1923 by Smekal(Smekal, 1923). In 1928, Raman and Krishnan observed Raman scattering for the first time using sunlight as a light source. The sunlight was put through a monochromator, then through a sample, and finally through a filter of a different wavelength than the original. If there was only elastic light scattering then all the light would the same as the incident rays, and thus unable to pass through the new filter. But some light was recorded on the receptor, meaning the sample change the light's energy levels. However, since the discovery of the phenomena, Raman spectroscopy was deemed too insensitive for chemical analysis due to strong florescence interference and weak intensity. From then until 1986 Raman spectroscopy studies were mainly physical and structural studies. By 1986, advancement in technology allowed for Raman spectroscopy to be a much more viable chemical analysis tool. The invention of Fourier transform (FT) Raman spectroscopy, small computers and near infrared lasers all contributed to the increased sensitivity of Raman by increasing the power and resolution of Raman scattering(McCreery, 2000) .

2.1.2. Principles

Light scattering is a daily occurrence that happens on the atomic scale. When molecules are hit with energy, such as sunlight, they are able to absorb some of the energy which causes vibration, stretching, and rotation. Upon relaxation, photons are

scattered from the sample. Most of the scattered photons are scattered elastically, meaning that the energy state of the scattered photon returns to the same state as the incident photon, which is called Rayleigh scattering. Elastic scattering is a result of the majority of the energy being scattered by the electron cloud. Since the electron cloud has such little mass, it does not absorb any energy and does not alter the energy state of photons. But every one in 10^6-10^8 photons are scattered inelastically, meaning something beyond the electron cloud has to affect the photons energy. The inelastic scattering is what is referred to as Raman scattering, and is caused by molecular motion beyond the electron cloud, into the structure of the molecule, and primarily the bonds. It is from this that Raman spectroscopy is founded on because of the difference in scattering among chemical bonds. (McCreery, 2000; Smith & Dent, 2005) For the spontaneous Raman scattering effect, the molecule will be excited from the ground state to a virtual energy state, and relax into a vibrational excited state, which generates Stokes Raman scattering. If the molecule was already in an elevated vibrational energy state, the Raman scattering is then called anti-Stokes Raman scattering (Figure 1). The shift in energy gives information about the phonon modes in the system.(McCreery, 2000)

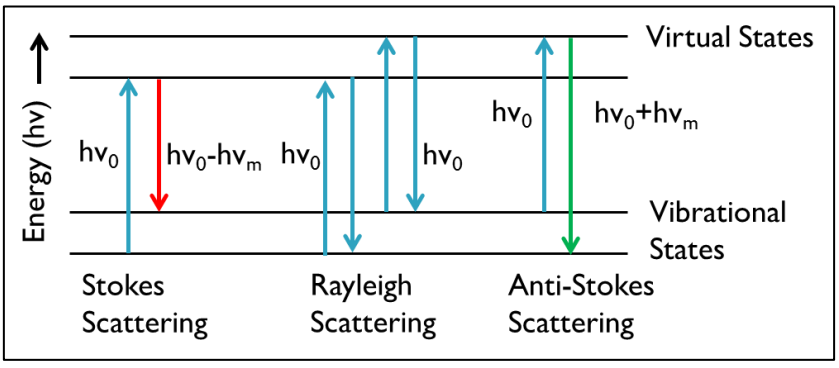

Figure 1: Schematic of stokes and anti-stokes Raman scattering compared to Rayleigh scattering.

2.1.3. Advantages

Being a vibrational spectroscopy, Raman spectroscopy is able to provide a unique spectrum for certain chemical groups due to inelastic photon scattering. Similar to infrared spectroscopy and NMR, each molecular bond is unique and can be characterized through the proper analysis. Raman spectroscopy has many useful advantages in food over similar techniques. First, it can measure a variety of samples, including the macronutrients, micronutrients and packaging materials that food comes in contact with. Next, it does not require a sample to be optically clear, because it does not require any light absorbance. This is paramount in the field of quality control where samples are tested for characterization and purity. Finally, a major advantage over IR spectroscopy is the strength of the water signal. IR spectroscopy provides a very strong water signal that must be subtracted from the total signal and can cause a major masking effect, whereas Raman spectroscopy has little-to-no water signal, providing no extra background noise.(Li-Chan, 1996) These advantages are more suited to the heterogeneity of a food system where many analysis techniques are not versatile enough to measure a sample *in vivo*, and must be broken down or prepared in a specific way.

2.2. Surface-enhanced Raman spectroscopy

2.2.1. What is SERS?

Raman scattering is inherently weak and has thus not been a major analytical tool compared to other techniques. However, it has been found that molecules adsorbed to certain metal nanostructures are capable of strengthening a Raman scattering signal. In 1974, Fleishman and others found that using a silver electrode in line with a Raman spectrophotometer which contacted a pyridine solution would greatly enhance the Raman signal, up to a million times(Fleischmann, Iiendra, & McQuillan, 1974). From their discovery, the concept of surface-enhanced Raman spectroscopy was founded and further investigated (Moskovits, 1985). The enhancement effect is mainly due to an electromagnet interaction of light with the noble metal. The result is an excitation referred to as a plasmon resonance. In order to induce the plasmon resonance(J. N. Anker et al., 2008; Jeffrey N. Anker et al., 2008), the sample must be within a maximum of 10nm from the surface of the noble metal. Additionally, when the space in between the nanostructures create a zone of very strong enhancement, referred to as a "hot spot" (Haynes, McFarland, & Duyne, 2005; Ru & Etchegoin, 2008).

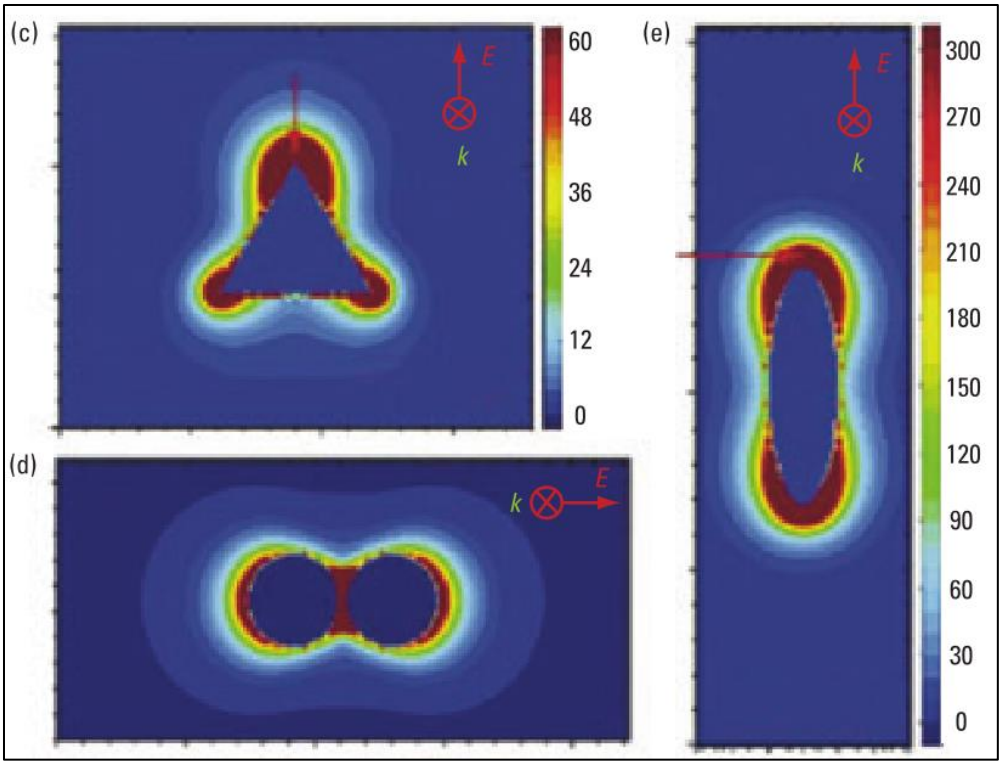

Figure 2: Illustration of the excitation of the localized surface plasmon resonances of various nanoparticles. Different shapes have different effects, as well as the space in between two nanoparticles. Haynes, 2005

2.2.2. SERS substrates

A good SERS substrate must be able to provide substantial enhancement of the Raman signal. The best and most common substrates for most applications are gold and silver nanostructures. Gold and silver work the best due to their optical properties, specifically at the visible and near-infrared range, common of Raman spectrophotometer lasers. The nanostructure is a conformation that increases surface area in order to ensure the contact between the metal and substrate. Nanoparticles are a common type of nanostructure, due to the requirement of a sub-wavelength particle. Nanoparticles tend to be 100nm or less, with no minimum. Roughened nanoparticles are beneficial due to the

even more increased surface area on the surface. Smooth surfaces and other metals may provide enhancement, but at a very low level.(Zheng & He, 2014)

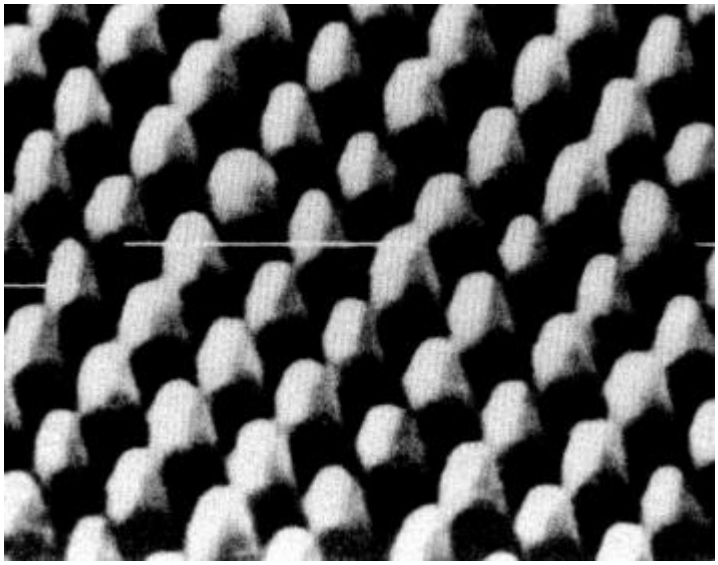

Figure 3: Electron micrograph of silver nanoparticle array, each post being about 100nm. Moskovits, 1985.

2.2.2.1. Gold nanoparticles

Gold nanoparticles are easy to make and only require three ingredients. The most common way of GNP production is using a bottom up method utilizing nucleation and growth(P. Zhao, Li, & Astruc, 2013). The three requirements for the synthesis is a gold precursor, a reducing agent and a stabilizing agent. Many methods have been developed for the creation of GNPs, but one of the most common methods is the Turkevich method(Kimling et al., 2006; Turkevich, Stevenson, & Hillier, 1951, 1953). The Turkevich method is rapid and reliable, using Chloroauric acid (HAuCl4) as the precursor and trisodium citrate dihydride as both the reducing and stabilizing agent. After the two are mixed, the nucleation phase can be seen by the change in color to a dark blue after 30 seconds of boiling, then the growth phase seen by the change in color to a bright

red after 90 seconds. The size of the GNP is dependent on the amount of sodium citrate added to the gold solution, with a size range from 16 nm to 147 nm.

Other ways of GNP synthesis include using alternate reducing agents such as hydroquinone or tannic acid and citrate as the stabilizing agent. It has also be shown that adding the gold to the citrate solution results in a smaller, more monodispersed GNPs.

Gold nanoparticles have taken a large role in delivery molecules for therapeutics and diagnostics. The gold core acts as a nontoxic source of structure and protection for a molecule to be delivered(Ghosh, Han, De, Kim, & Rotello, 2008; Kong, Bae, Jo, Kim, & Park, 2011; Niidome et al., 2006).

The size of gold nanoparticles is important to know and monitor. The most accurate way of measuring the size of nanoparticles is by using an electron microscope, such as an SEM or TEM. However, using a UV-Vis spectrophotometer to measure the absorbance or chrominance of the nanoparticles can be used to correlate the size(Jing et al., 2012; Njoki et al., 2007). Optical spectroscopy has been used to analyze the local plasmon resonance of a nanoparticle, which is of fundamental importance in SERS(Prikulis et al., 2004).

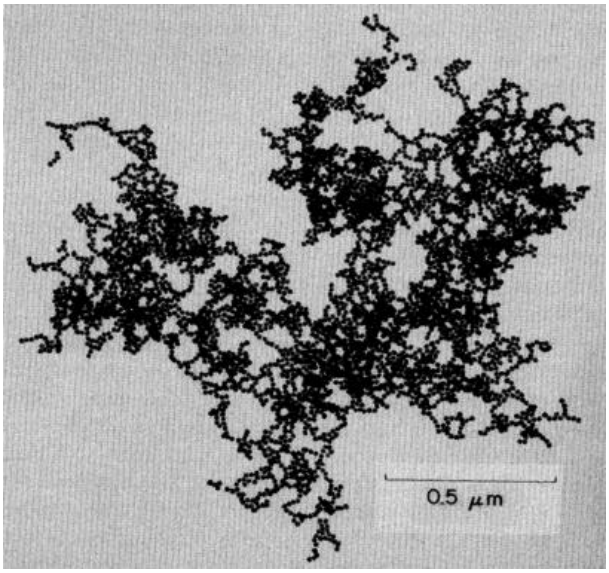

Figure 4: SEM image of colloidal gold nanoparticles aggregating together. Moskovits

2.2.2.2. Modification of gold nanoparticles

An interesting property of the GNPs is the ability to be modified with different ligands, particularly alkanethiols, to create a monolayer around the GNP. The thiol group has a high affinity to gold, a covalent bond almost as strong as a gold-gold interaction, which why it acts as a good ligand group to modify the surface properties of the GNP(Fendler, 2001; Giersig & Mulvaney, 1993; Häkkinen, 2012; Hinterwirth et al., 2013; Hostetler, Stokes, & Murray, 1996; Jadhav, 2012; Kyrychenko et al., 2012; Lau et al., 2011; Love, Estroff, Kriebel, Nuzzo, & Whitesides, 2005; Nuzzo & Allara, 1983; Pieters & Prins, 2012; Porter, Bright, Allara, & Chidsey, 1987; Rana, Bajaj, Mout, & Rotello, 2012; Rasch, Bosoy, Yu, & Korgel, 2012; Rasch, Yu, Bosoy, Goodfellow, & Korgel, 2012; Rasch et al., 2010; Sekiguchi, Niikura, Matsuo, & Ijiro, 2012; Simard, Briggs, Boal, & Rotello, 2000; Swami, Kumar, Selvakannan, Mandal, & Sastry, 2003; Tam et al., 2012; Tessier et al., 2002; Thomas, Zajicek, & Kamat, 2002; Weisbecker et

al., 1996). Because GNPs are made in a citrate buffer, they are quite hydrophilic and immiscible in organic solvents or lipid systems. In order to increase they hydrophobicity they must be modified with a ligand.

One way modified GNPs have been used is as a delivery system that is resistant to macrophage uptake. The monolayer acts as a hydrophobic barrier that the macrophage cannot adhere to.(Larson, Joshi, & Sokolov, 2012)

Brust and others have devised a direct synthesis method for modified GNPs(Brust, Walker, Bethell, Schiffrin, & Whyman, 1994). The method utilized the aqueous phase of the gold and an organic layer of toluene and octanethiol. The major addition to this synthesis is tetraoctylammonium bromide (TOAB) which acts as a phase transfer agent, which allows all of the molecules to interact. The reducing agent is added and vigorous mixing is required for 3 hours, which then results in 1-3 nm GNPs with octanethiol conjugated on the surface.

2.2.2.3. Silver dendrites

Silver dendrites are an economical and easy to use SERS substrate. They provide a large roughened surface area for excellent Raman enhancement. He *et al* describe the method for preparing silver dendrites. Silver nanostructures were prepared via a simple replacement reaction involving both zinc (Zn) and silver nitrate (AgNO3): Zn+AgNO3 →Ag+ZnNO3. First, an aqueous solution of silver nitrate was prepared by dissolving AgNO3 in deionized water. A solid zinc plate was first cleaned by dilute hydrochloric acid (0.02mol/l) to remove surface contamination, and then rinsed with deionized water, followed by drying with cold air. The zinc plate was then immersed into the AgNO3

solution. Silver nanostructures with different morphologies are able to be obtained quickly by adjusting the silver ion concentrations. The nanostructure products were carefully peeled off the zinc plate with tweezers and put into a glass bottle. The nanostructure products were then rinsed several times using deionized water to remove excessive chemicals like Zn2+ and NO3−.(He, Haynes, Diez-Gonzalez, & Labuza, 2011; He, Lin, Li, & Kim, 2009).

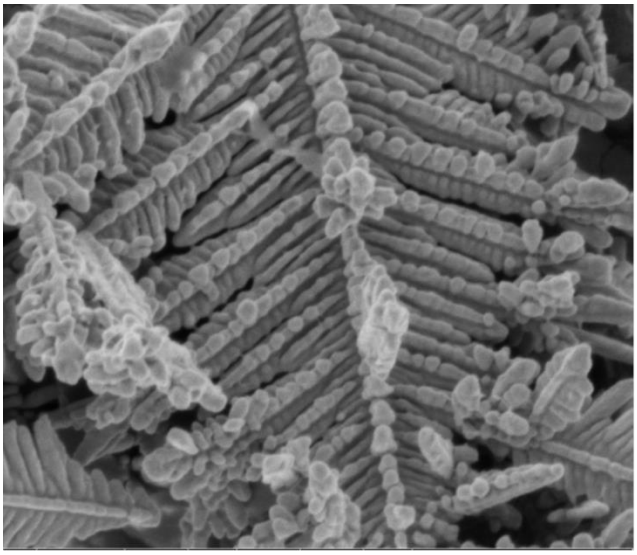

Figure 5: SEM image of silver dendrites, being about 1um at the top of the image. The coarse structure leads to better SERS enhancement of substrates.

2.2.3. SERS application in food science

SERS has been used in many different fields to rapidly measure and detect minute amounts of a substrate. The SERS technique has become much more popular in food science in recent years, with almost 60 cited scientific journal articles using SERS in food related studies in 2013 alone. The existing research identifies and characterizes various chemical substrates including food additives, contaminants, adulterants and microbiological substrates. Food contaminants include pesticides (Pang, Labuza, & He,

2014), antibiotics and other illegal drugs, melamine(Y. Zhao et al., 2013), illegal food colors, mycotoxins and foreign allergenic protein toxins. (Zheng & He, 2014)

In addition to chemical contamination, there are numerous studies applying SERS to food related microbiological detection, since food borne illness is a major concern in the food industry. Traditional testing for pathogenic contamination in food requires culturing of the sample and allowing sufficient time for the bacteria or mold grow. SERS techniques have been developed to eliminate the culturing time by detecting very small amounts of pathogens.(Craig, Franca, & Irudayaraj, 2013) Other biological material, such as pollen, have been subject of SERS measurement as well (Sengupta, Laucks, & Davis, 2005).

Beyond the major food applications of SERS, hydrophobic applications have been successful in other fields. SERS has been used to detect the presence of contaminants in water with cystamine modified GNPs(Ruan, Wang, & Gu, 2006). Gold nanoparticles have been used to enhance very low concentrations of the antioxidant BHA(Yao et al., 2011) and essential oils of plants(Rösch, Popp, & Kiefer, 1999). SERS has becoming more popular in the biomedical fields due to the ability to enhance low concentrations, down to individual molecules(Kneipp, Kneipp, Itzkan, Dasari, & Feld, 1999). One area of SERS research is immunoassays(Porter, Lipert, Siperko, Wang, & Narayanan, 2008). GNPs are modified with antibodies or aptamers which can bind to specific targets, which can then be measured with SERS(Pang et al., 2014).

Additionally, a study by Yang *et al* performed a study on folic acid and methotrexate using two SERS substrate(J. Yang et al., 2014). The experiments utilized a copper foil foundation with silver nanoparticles as a secondary nanosubstrate added on

top of the copper foil for a "sandwich" effect. Using the two noble metal substrates strengthened the enhancement effect of the Raman signals significantly.

2.3. Current analytical challenges for emulsion and lipid analysis

2.3.1. Current techniques for characterization of emulsions and their limitations

There are numerous factors to consider when characterizing emulsions, including particle size, charge, type (o/w w/o) and composition. A major component of the emulsion is the interfacial region, despite having a small overall volume it has a major effect on the whole emulsion. The interfacial composition can affect the emulsion significantly including particle size, stability, susceptibility to lipid oxidation and digestion. Some properties of an emulsifying agent include structure, charge, energy, and rheology. Because the interface is such an important area of an emulsion, it is desirable to characterize it. Some techniques include light scattering and reflection, microscopy and spectroscopic such as infrared and fluorescence. However, there is a lack of techniques that provide *in situ* characterization of the interfacial region.(McClements, 2004)

2.3.2. Current lipid oxidation detection methods and their limitations

Lipid oxidation is a major quality control concern in the food industry. Not only does lipid oxidation produce volatile compounds responsible for perceived rancidity, but it also deteriorates the quality of the lipid composition. Polyunsaturated fatty acids are generally considered the healthy type of fatty acid, but due to their structure they are the most susceptible to lipid oxidation and the first to oxidize.(Damodaran, Parkin, & Fennema, 2007)

Lipid oxidation is a free radical processes which is accelerated by heat, oxygen presence and heavy metal presence. The more unsaturated a fatty acid is, the quicker it oxidizes. If a fatty acid has at least two double bonds, the first step is the formation of conjugated double bonds (conjugated dienes). Next is the formation of peroxyl radicals, and hydro peroxides. After that, secondary products are formed through beta-scission. Secondary products can be aldehydes, ketones, alkanes and short chain fatty acids; all of which are volatile.

There are a number of traditional methods that can measure lipid oxidation, which utilize the measurement of products from various stages of oxidation. Single product measurements include spectroscopic methods of lipid hydro peroxides and conjugated dienes(Kittipongpittaya, Chen, Panya, McClements, & Decker, 2012; Laguerre et al., 2011). Chromatography methods can be used to measure multiple products from lipid oxidation, which includes hexanal measurement from gas chromatography. Each method has their own benefits. Individual product measurements are quick and many duplicates can be run. But since they only measure for one product, other tests need to be run alongside of it. Chromatographic methods are able to measure for multiple products, but they require a lot of time to run.

Emulsions are an important part of the food industry. Because one of the major constituents is an oil, oxidation is a concern(Hu, McClements, & Decker, 2003; Jacobsen et al., 2000; Tsuzuki et al., 2004). The reaction is complex due to the different phases, the interface and different prooxidants and antioxidants present in either phase. Besides the basic factors of lipid oxidation, emulsions have other considerations. For example, at the interfacial layer can vary in composition, thickness, charge and permeability.

Additionally, droplet size and concentration has an effect on the rate of oxidation(Waraho, McClements, & Decker, 2011).

Although not a traditional technique, there was a method established relying on a chemical reaction of triphenylphosphine (TPP) measured by IR spectroscopy(Ma et al., 2000). TPP undergoes an oxidation reaction when in contact with hydroperoxides. Triphenylphosphine oxide (TPPO) provides a different signal under IR than TPP, so the change in spectra can be monitored to correlate the amount of hydroperoxides. This method was established for sulfonated oils in the leather industry, but the principle can be translated for other applications.

2.4. Current application of Raman with lipids

Raman spectroscopy has already proved itself useful for measuring different lipid samples. A study done by Baeton and others classifies 21 different types of oils and fats based on their Raman signal proving the relative sensitivity of the technique for food lipids (Baeten & Hourant, 1998; Sadeghi-Jorabchi, Wilson, Belton, Edwards-Webb, & Coxon, 1991). Their classification has also created a foundation of Raman shift classification, as seen in Table 1. Furthermore, Raman spectroscopy was able to determine presence of hazelnut oil and olive pomace oil in adulterated olive oil which is an adulteration concern in the food industry (Baeten et al., 2005; H. Yang & Irudayaraj, 2001). These studies are important to show the accuracy of Raman signals in differentiating different types of similar oils. In more complex food systems, Raman has been able to determine the CLA content in milk was able to be measured using Raman signals(Meurens, Baeten, Yan, Mignolet, & Larondelle, 2005). SERS has also been used

in lipid samples, particilarly films and bilayers(Chua, Chapman, & Stachowiak, 2012; Heywang, Saint-Pierre Chazalet, Masson, & Bolard, 1998). One of the most popular areas of lipid chemistry is measuring lipid oxidation, which has been measured with Raman spectroscopy. The studies done by Muik *et al* were done on oil oxidized at 160^{o} for 9 hours. The rapid oxidation test was analyzed with an FT-Raman. The results show a change in peaks over time and some characterization includes an increase in carbonyl groups, an increase in trans double bonds and an increase in conjugated dienes. (Muik et al., 2005; Sweetenham & Notingher, 2010; Weldon, Zhelyaskov, & Morris, 1998). Based on the previous Raman data from food lipids, general peak assignments can be made.

Raman Shift (cm-1)	**Assignments**
3015	=C-H, Asymmetric
2970-2940	-C-H, Asymmetric
2900-2860	-C-H, Symmetric
1700-1750	C=O
1670	C=C, Trans
1660	C=C, Cis
1445	C-H
1310	C-H
1275	=C-H, Cis
1100-800	C-C

Table 1: Raman shift assignments, adapted from Baeton *et al* (Baeten & Hourant, 1998).

2.5. Objectives of this study

2.5.1. Amphiphilic GNPs for emulsion interface characterization

The objective of this experiment was to produce a gold nanoparticle that will adhere to the interface of an emulsion to enhance the interfacial layer *in situ*. With the GNPs at the interface they will enhance the signal of the material in close proximity, being the emulsifier in this case. Then SERS measurements can be taken to observe the interfacial layer of the emulsion rapidly and without breaking the emulsion down.

2.5.2. TPP chemical reaction to rapidly measure peroxide values

The objective of this experiment was to utilize the chemical reaction of TPP to TPPO when in contact with peroxides using normal Raman spectroscopy. Although it measures only one product of lipid oxidation, Raman spectroscopy is much quicker than traditional peroxide tests. Additionally, Raman spectroscopy may be a better method than the established IR method in food systems based on the fundamental principles.

2.5.3. Lipophilic GNPs for lipid oxidation study

The objective of this experiment was to produce hydrophobic GNPs that were soluble in an organic solvent, such as hexane. With hydrophobic GNPs mixed with a food oil, the SERS enhancement can be greater than the substrate SERS method as well as increasing enhancement for low concentration oxidation products. Having the ability to use SERS to enhance food oils would increase the speed and sensitivity for lipid oxidation detection.

2.5.4. Modification of SPME fibers with GNPs for detection of volatile compounds using headspace SERS

The objective of this experiment was to capture and characterize the volatile compounds released from lipid oxidation. Since many oxidation products are volatile and cannot be detected easily using typical SERS methods, a method needs to be created for volatiles. This method combines SERS techniques and gas chromatography techniques to create a simple and rapid method for volatile detection and characterization.

2.5.5. SERS measurement of canola oil using Ag dendrites

The objective of this study was to utilize silver dendrites to enhance canola oil signals. The substrate method for SERS is the most easily prepared method making it very simple, cheap and rapid. Using the enhancement from the silver dendrites, the secondary objective was to monitor the oxidation process of canola oil using the substrate method for simple and rapid detection of lipid oxidation products.

2.5.6. SERS measurement of canola oil using the sandwich method

The objective of this study was to combine the hydrophobic GNP technique with the silver dendrite method. The combination of two SERS substrate allowed for a higher contact area and theoretically, a higher enhancement level. Using the two methods as one, the consistency should have been better than each individual method.

2.5.7. Novelty of our approaches

SERS has only recently become a more common analytical tool in food science. It

offers a more rapid and inclusive set of data than traditional techniques. Modification of GNPs has been done, but never for SERS application in food. Previous modifications have included compounds that provide a strong Raman signal and thus background noise that would interfere with sample readings. Additionally, SERS has not been used to measure lipids or emulsions. The modified GNPs can be mixed into the appropriate mixtures and enhance Raman signals from the canola oil or emulsion interface, which has not been done before. The TPP chemical reaction was done using IR previously, but using it for Raman spectroscopy will bring more viability and wider array of application than just IR. Having a foundation for different Raman and SERS techniques can lead the way for more applications which increase the speed and sensitivity of analytical testing.

CHAPTER 3

MATERIALS AND METHODS

3.1. Fabrications of GNPs in citrate buffer

The method used for synthesizing gold nanoparticles for the following experiments was the Turkevich method. The method is a reduction of gold chloride (HAuCl4) with trisodium citrate (Na3Cit) in an aqueous solution. The citrate also acts as a capping agent for stabilizing the GNPs.(Frens, 1973; Turkevich et al., 1953) The glassware used for the production of GNPs was treated with aqua regia to clean the glass of any impurities. First, the gold chloride was made into a 0.1% solution by weight with water and heated to a boil. Next, a 1% solution of sodium citrate was rapidly injected into the gold chloride solution. The amount of the sodium citrate added controls the size of the nanoparticles formed: A higher amount of sodium citrate will result in smaller nanoparticles whereas less added will result in larger nanoparticles. The standard size produced for this method was for 42nm particles, and 0.1% NaCit, or 500ul per 50ml. The nanoparticles differ in color along with their size; the larger ones being a dark red to a violet color, and the smaller ones being more of a bright red to orange. The nanoparticles were left to cool at room temperature, and then transferred into a closed container.

3.2. Modification the hydrophobicity of GNPs

3.2.1 Amphiphilic GNPs

Gold nanoparticles were placed in a 50 ml plastic tube. Next, an equal amount of 5% octanethiol in hexane was added. The mixture was left to mix on a Nutating Mixer (Fisher Scientific) for 12 hours. The nanoparticles then accumulated at the interface between the citrate buffer and hexane and were extracted into another container.

3.2.2 Lipophilic GNPs

GNPs were placed in a 50ml plastic tube. Next, an equal amount of 5% octanethiol in 2-propyl alcohol was added. 2-propyl alcohol was added because its polarity is in the middle of water and hexane, for optimal interaction with the GNPs. The mixture was left on a molecular devices rotator for 60 hours. Next, the mixture was homogenized with a trumixer4000 (Fisher Scientific) for 3 minutes. Finally, the GNPs were extracted with the hexane into a separate container. For best results, the modified GNPs were sonicated (Sonic dismembrator, Fisher Scientific) before use.

After time the hydrophobic GNPs would stick to the walls of the glass container, which were not able to be retrieved. To overcome this, the glassware was treated with piranha solution(Lohbauer, Zipperle, Rischka, Petschelt, & Müller, 2008; Touzi et al., 2006). The piranha solution, which is a mixture of hydrosulfuric acid and hydrogen peroxide, is capable of hydroxylating the glass surface, making it more hydrophobic and thus resistant to the hydrophobic GNP interaction. It should be noted than piranha is a very dangerous solution, and extreme caution must be taken when preparing and using it.

3.3. Characterization of GNPs

3.3.1 Size distribution

The original aqueous GNPs were analyzed using a zetasizer nano (Malvern). One ml of sample was placed into a plastic cuvette and was run in triplicates. The refractive index used was set to 2.4. Both of the modified nanoparticles did not provide sufficient measurements due to aggregation, according to the software. Additionally, the cuvette started to crack due to the octanethiol.

3.3.2 TEM

Each of the GNPs was imaged using a JEOL JEM-2000FX transmission electron microscope to analyze their shape and size with the assistance from the UMass Electron Microscopy Center. Five microliters of sample was placed onto a carbon coated copper mesh (Electron Microscopy Sciences, Hatfield, PA) for TEM imaging.

3.3.3 Raman

Each of the GNPs was analyzed using a Raman spectrophotometer (Thermo Scientific DXR Raman microscope, 734 nm laser, 5mW). 20 microliters of each sample were placed onto a gold slide then left to dry and measured.

3.3.4 UV-Vis Spectroscopy

A Molecular Devices Spectramax M2e spectrophotometer was used to measure the absorbance of the different nanoparticles in a Falcon 96 well plate. A wavelength scan was used to determine the absorbance peaks, with 10nm intervals. The literature

shows that colloidal GNPs have an absorbance peak at 520nm. When the surface charge is removed, typically due to binding of a surface ligand, the GNPs are able to aggregate causing a very broad peak at 700nm. (Shi, Zhao, Liu, Fan, & Cao, 2013)

3.4. Applications of amphiliphic GNPs in emulsions

3.4.1 Emulsion preparation

An oil-in-water emulsion was made, with 10% oil as the dispersed phase. B-lactoglobulin was used as an emulsifier, in varying amounts. The amphiliphic GNPs were mixed with the aqueous phase along with the BLG. After the oil was added, the mixture was homogenized with a Powergen 125 homogenizer (Fisher Scientific) for 1 minute.

3.4.2 Emulsion characterization

The emulsion was placed under the Raman microscope (Thermo Scientific DXR Raman microscope, 734 nm laser, 5mW). Raman spectra were taken from the emulsion with and without the nanoparticles.

3.5. Applications of Raman spectroscopy and SERS in lipid oxidation study

3.5.1. Design of lipid oxidation study

33 glass vials containing 1 ml of canola oil each were incubated at 55^{o}C for 10 days. Each day at the same time, three vials were taken out and measured using conventional lipid oxidation techniques and SERS using the oil enhancement procedure.

3.5.2. Detection of lipid oxidation products using conventional techniques

Each day three vials were taken out of the incubator in order to run triplicates. The first test was the hexanal test using a GC-17A Shimadzu gas chromatograph equipped with an AOC-5000 autosampler (Shimadzu, Kyoto, Japan). Samples (1 mL) in 10-mL glass vials capped with aluminum caps with PTFE/silicone septa were preheated at 55 °C for 15 min in an autosampler heating block. A 50/30 lm DVB/Carboxen/PDMS solid-phase microextraction (SPME) fiber needle from Supelco (Bellefonte, PA) was injected into the vial for 2 min to absorb volatiles and then was transferred to the injector port (250 °C) for 3 min. The injection port was operated in split mode, and the split ratio was set at 1:5. Volatiles were separated on a Supleco 30 m 9 0.32 mm Equity DB-1 column with a 1 lm film thickness at 65 °C for 10 min. The carrier gas was helium at 15.0 mL/min. A flame ionization detector was used at a temperature of 250 °C. Hexanal concentrations were determined from peak areas using a standard curve prepared from authentic hexanal.

The second test was the peroxide value. Lipid hydroperoxides were measured using a method adapted from Shanta and Decker [25]. The bulk oil samples (20 uL) were weighed accurately and then 2.8 mL of methanol/butanol solution (2:1, v/v) was added followed by the addition of 15 uL of 3.94 M ammonium thiocyanate and 15 lL of 0.072 M ferrous iron solution (prepared by mixing 0.132 M BaCl 2 and 0.144 M FeSO 4). The 123J Am Oil Chem Soc absorbance of the samples was measured at 510 nm using a Genesys 20 spectrophotometer (ThermoSpectronic, Waltham, MA) 20 min after the addition of the iron. The concentration of hydroperoxides was calculated

from a cumene hydroperoxide standard curve.

Finally conjugated dienes were measured. Weighted oil samples were dissolved in iso-octane at the appropriate dilution factor, and conjugated diene absorbance was measured at 234 nm in a Shimadzu spectrophotometer (UV- 2101PC, Shimadzu, Kyoto, Japan).

3.5.3. Detection of lipid oxidation products using normal Raman based TPP chemical methods

400ul of pure canola oil was placed into an Eppendorf tube and 24ul of saturated TPP in chloroform was added. The mixture was vortexed for 20 seconds then left to mix on the nutating mixer (Fisher Scientific) for 30 minutes. 300ul of the mixture was added into a well of a 96 well plate. The plate was then placed under the Fisher DXR Raman microscope and read. Because the test was only using normal Raman, full laser power (24mW) was used. Conventional peroxide value testing was run alongside of this experiment, according to section.

3.5.4. Enhancing lipid signals using hydrophobic GNPs

Due to the high amount of GNPs needed for the solution method, oil was diluted to 3% using the GNP mixture as the diluent. 20ul of the mixture was then placed on a gold slide and left to dry. When using the Raman microscope, dark spots of aggregated GNPs were selected for their hotspot properties.

3.5.5. Detection of lipid oxidation products using SERS with lipophilic GNPs

The modified GNPs were sonicated and used to dilute store bought canola oil to 3%. The samples were left to mix on a fisher Nutating mixer for 5 minutes. A control sample of 3% oil in hexane was also prepared. The GNP and oil sample was mixed and 20 ul were immediately placed on a gold slide and left to dry. 20 ul of the 3% oil in hexane was also placed on the slide. When fully dried, the samples were measured using a Fisher DXR Raman microscope.

A preliminary oxidation trial was used for validation of the method. It started at day 0 and ended at day 7 at with the oil being incubated at 55^{o}. The oil enhancement procedure was used to observe the differences at the beginning and the end of the trial to start characterizing the changes caused by lipid oxidation. Then, a kinetic trial was performed with 30 samples points were taken each day and Omnic software was used to compile the spectra and TQ Analyst software was used to analyze the data.

3.5.6. Detection of volatile lipid oxidation products using gold modified steel wire

40um diameter steel wire was cut into 5cm segments. They were submerged into a solution of gold chloride as a pretreatment. They were then rinsed with deiononized water. Next, they were submerged in a 1% octanedithiol – ethanol solution for 12 hours. The wires were then rinsed with ethanol. Then they were submerged in GNPs for 48 hours. The octanedithiol and GNP steps were repeated six times.

The viability of the headspace enhancement was tested with two lipid oxidation control products: hexane and hexanal. Hexane is more hydrophobic and hexanal is more hydrophilic, so it tested two different types of products. 100 ul of the sample was placed

in a sealed glass vile with the modified steel wire seals in the top of the vile. It was incubated at 55^{o}C for one hour. The wire was removed and tested under the Raman microscope.

The setup was the same as the other lipid oxidation trials: 15 vials with 200ul of canola oil each were placed in the incubator at 55oC for 14 days. On each day, a vial of oil was taken out of the incubator and placed in the freezer for one hour in order to reduce the volatility of the oxidation compounds. The vials were opened and the wire was inserted in the cap without touching the oil, and sealed again. The vial of oil was then placed in the incubator at 75oC for one hour. Finally, the wire was taken out, put on a glass slide and analyzed under the Raman microscope.

5.5.7. Detection of lipid oxidation products using SERS with silver dendrites

Silver dendrites were produced using the displacement method using zinc and silver nitrate. 3 ul of silver dendrites were deposited onto a glass slide and let to dry. 10 ul of sample was placed on top of the silver. The Raman DXR microscope was set to 5 mW using the 10x objective.

In order to test for lipid oxidation using this method, 1 ml of canola oil was placed into 25 ml sealed vials, totaling 10 vials. One vial was removed every 24 hours and let to cool, then diluted to 3% with hexane for analysis.

3.5.8. Enhancing lipid signals using the sandwich method combining hydrophobic GNPs and silver dendrites

This method was similar to the normal hydrophobic GNP enhancement method.

However, instead of placing the GNP and oil mixture on a gold slide, the mixture was placed on a spot of silver dendrites. The canola oil was diluted to 3% concentration in the hydrophobic GNPs and mixed. Then, the mixture was place on the silver dendrites and left to dry.

CHAPTER 4

RESULTS AND DICSUISSION

4.1. Fabrication and Modification of GNPs

Following the citrate reduction of gold chloride as characterized by Frens, gold nanoparticles were produced. After heating the gold chloride solution, the sodium citrate was added. After 30 seconds the solution turned a dark blue color, which is the nucleation phase. After 60 seconds the solution turns red, which is the growth phase.

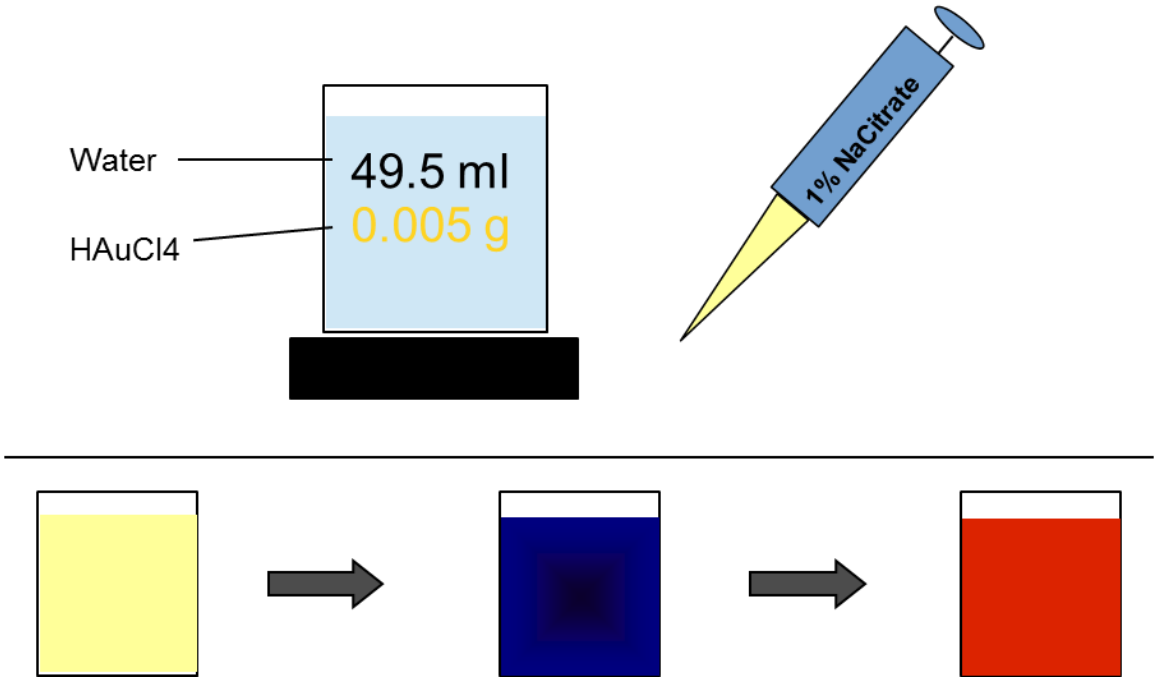

Figure 6: A schematic diagram of the creation of GNPs in an aqueous citrate buffer. The pale yellow 0.01% HAuCl4 solution quickly turns a dark blue color after the addition of 1% NaCitrate. It then turns to a dark red color indicating the completion of the reaction.

4.1.1. Modification of Amphiliphic GNPs

The GNPs were mixed in a solution of hexane and octanethiol. Because of the difference in polarity, the GNPs did not mix with the hexane solution. But after given

enough time and mixing the particles aggregated at the interface of the aqueous buffer and the hexane. It was considered a partial modification as only part of the particle's surface was in contact with the octanethiol.

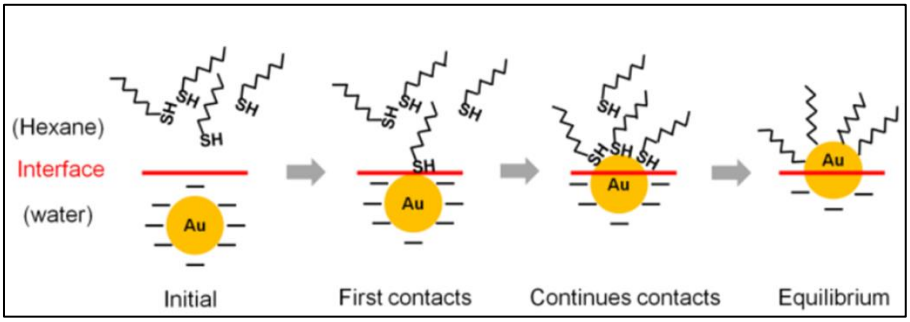

Figure 7: Schematic diagram of the modification of amphiliphic GNPs. Because hexane and the citrate buffer are immiscible the octanethiol cannot fully attach to the GNPs resulting in a partial modification.

4.1.2. Modification of Hydrophobic GNPs

Because of the known spontaneous interaction between thiols and gold, the GNPs were mixed with octanethiol with isopropyl alcohol as an intermediate solvent for full contact and conjugation of the octanethiol. After the mixing and extraction, the GNPs would settle to the bottom of the container and would need sonication to be dispersed.

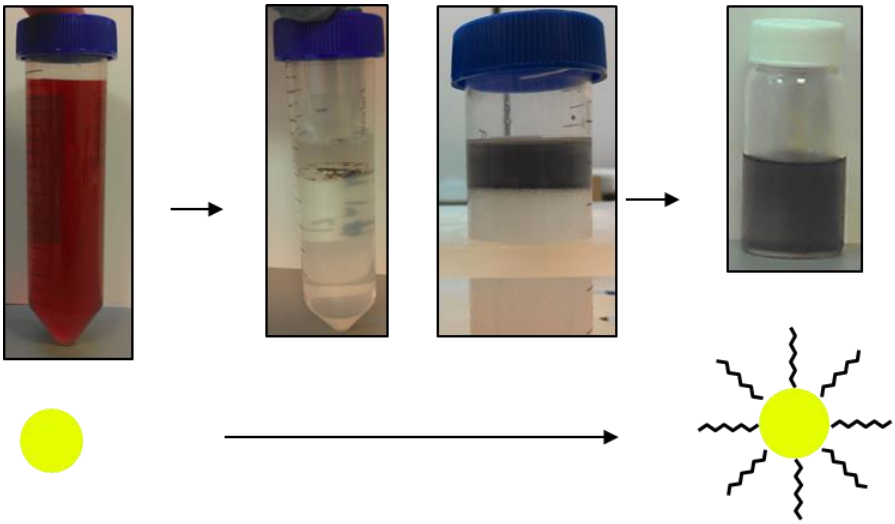

Figure 8: The modification of GNPs with octanethiol. A, Hydrophilic GNPs. B, After

mixing with octanethiol and IpOH and addition of hexane. C, After homogenization. D, Extraction of hydrophobic GNPs

4.1.3. Purification of Hydrophobic GNPs

Due to the excess octanethiol used to ensure full modification of the GNPs, there was free octanethiol in the hexane which may interfere with the Raman signal. Simple evaporation and addition of hexane three times helped remove the excess octanethiol.

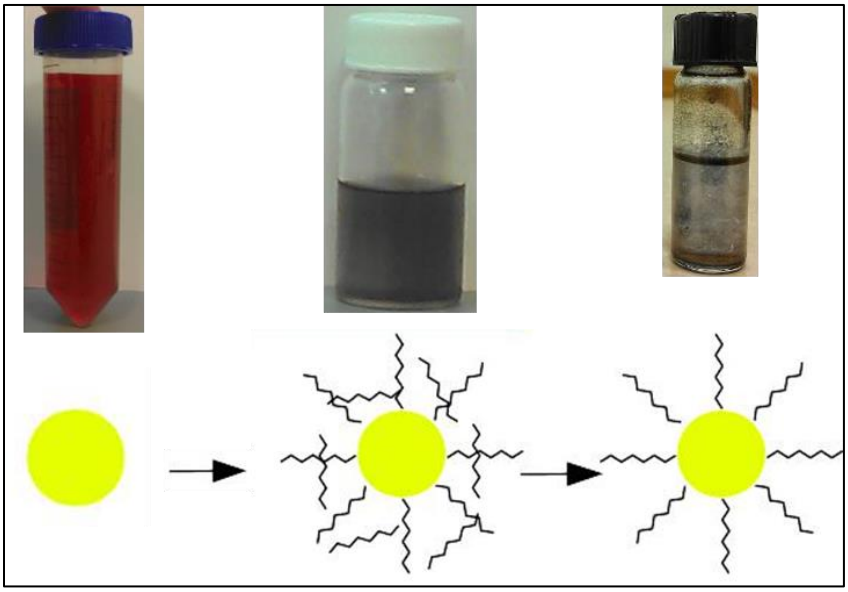

Figure 9: Macroscopic pictures and graphical representations of hydrophilic GNPs, the modification with octanethiol and the purified GNPs to rid the free octanethiol from the system.

4.2. Characterization of GNPs

4.2.1. Size Distribution

The zetasizer provided size distribution data. There was a strong peak around 30nm but the sizes ranged from 10 to 50 nm.

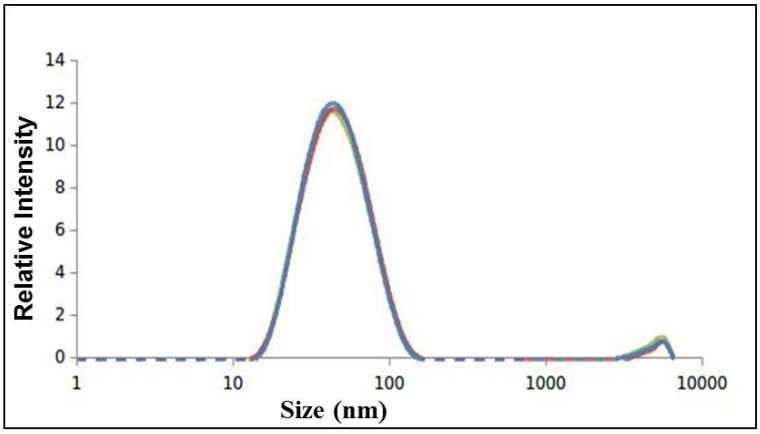

Figure 10: GNP size distribution from the Zetasizer nano

4.2.2. TEM Images

Hydrophilic TEM

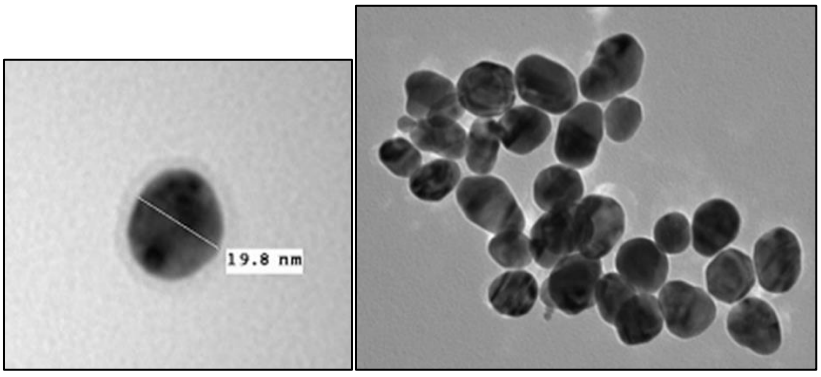

Figure 11: TEM images of colloidal hydrophilic GNP a) with size label and b) aggregate

Hydrophobic TEM

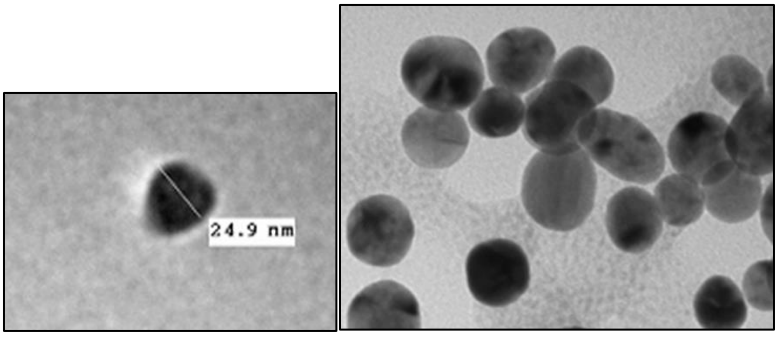

Figure 12: TEM images of colloidal hydrophobic GNP a) with size label and b) aggregate

4.2.3. Raman Signals from GNPs

The hydrophilic GNPs have characteristic Raman peaks primarily from the citrate capping agent. There is a bread peak from 3100 cm-1 to 2800 cm-1. There are also a handful of peaks from 1500 cm-1 down to 400 cm-1. The peaks are from C-C stretching, C-H stretching and C=O stretching.

After modifying the amphiphilic GNPs some changes in the Raman spectra were apparent. The spectra for the amphiphilic GNPs have increased peaks at 2883, 1465, 1305 and 1070 cm-1 which can be attributed to C-C and C-H stretching from the conjugation of octanethiol.

After a full modification of the hydrophobic GNPs with octanethiol, there were different Raman peak changes. There was an increase in peak 1070 cm-1 with the added octanethiol which can be attributed to the C-C stretching, and a decrease at peak 700 cm-1. With the addition of the purification step the peaks did not change any more from the original hydrophobic GNPs, just increased the intensity and resolution of them.

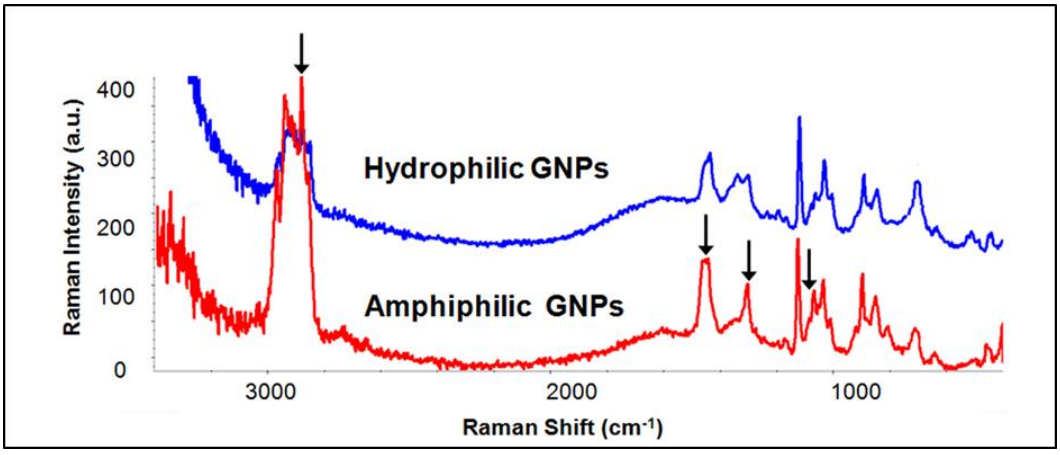

Figure 13: Raman spectra of GNPs before (hydrophilic) and after modification (amphiphilic). The spectra for the amphiphilic GNPs have increased peaks at 2883, 1465, 1305 and 1070 cm-1 which can be attributed to C-C and C-H stretching from the conjugation of octanethiol.

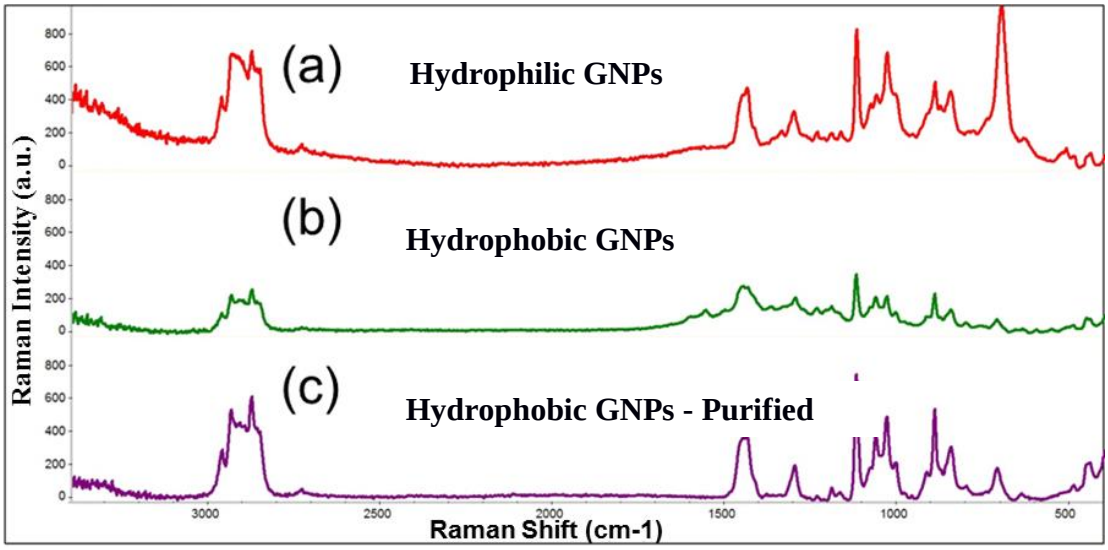

Figure 14: Comparison purified GNPs. (a) GNPs provide a characteristic signal, based on the citrate capping agent. (b) The modified GNPs have additional peaks from the octanethiol from the extra C-C and C-H bonds. (c) The purified hydrophobic GNPs have the same spectra as the previous sample

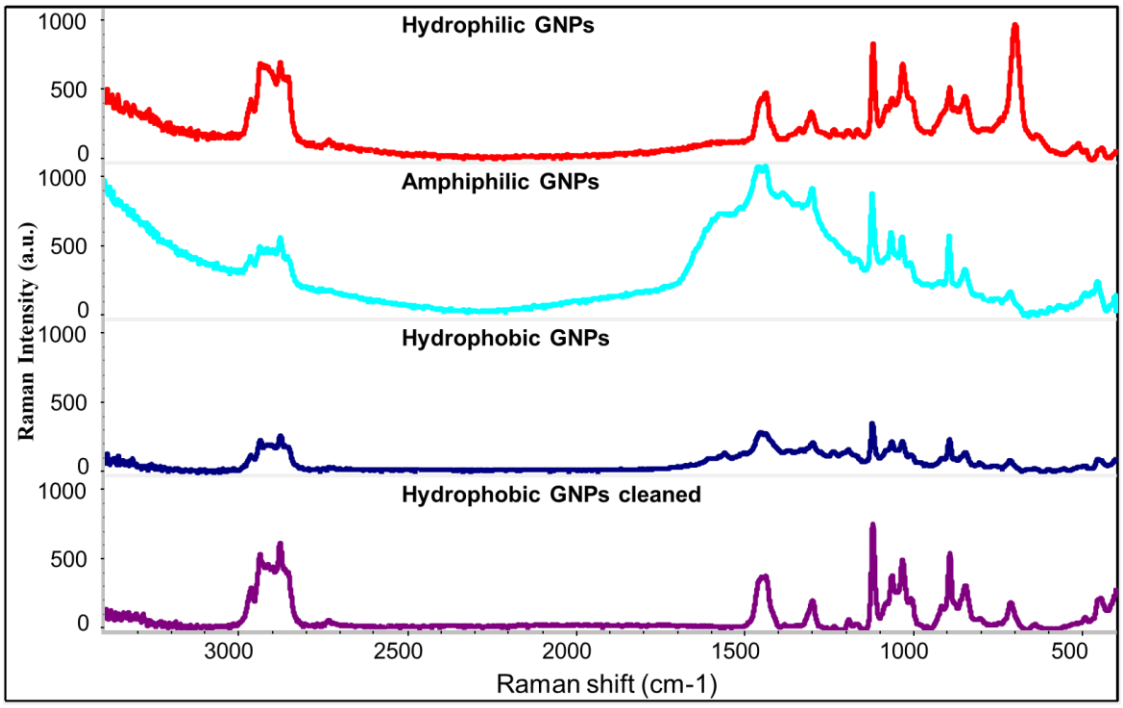

Figure 15: Hydrophilic GNPs compared to amphiphilic GNPs, hydrophobic GNPs and the purified hydrophobic GNPs which shows the similarities and differences with the modifications.

4.2.4. UV Vis Absorbance

The UV-Vis spectra were taken for the hydrophilic GNPs and hydrophobic GNPs. The spectra could not be taken for the amphiphilic GNPs because they were not fully dispersed throughout a single solvent. The spectra for the hydrophilic GNPs had a peak at 525nm whereas there was a broad peak for the hydrophobic GNPs from 500 to 675. There may have been some settling with the hydrophobic GNPs.

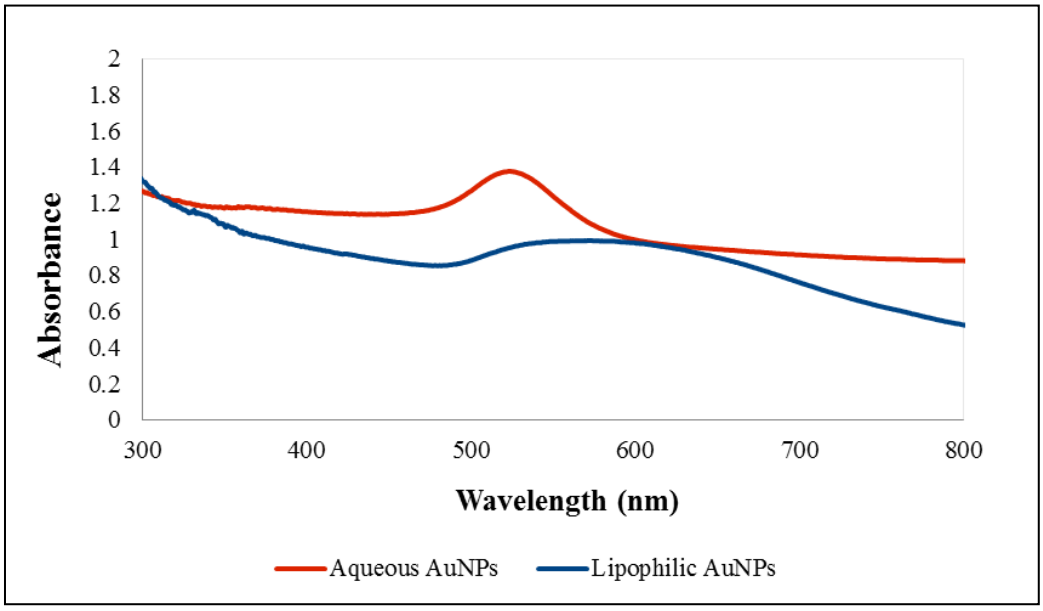

Figure 16: UV-Vis absorbance of hydrophilic and hydrophobic GNPs. The hydrophilic GNPs have a peak at 525 nm and the hydrophobic GNPs have a broad peak from 500 to 675.

4.3. Emulsion Analysis

To prove that the GNPs can enhance the emulsifier, a control was tested. BLG in solution was prepared with GNPs in both 10% and 1% concentrations. As shown in Figures 6 & 7, enhancement was possible.

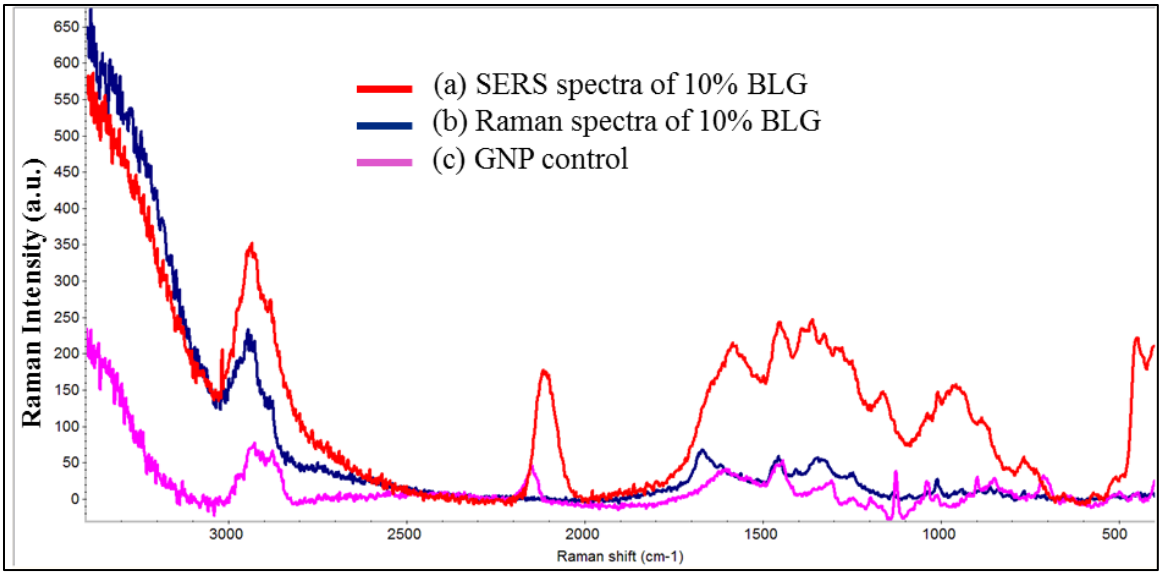

Figure 17: (a) SERS spectra of 10% BLG solution. (b) Raman spectra of 10% BLG solution. (c) GNP control.

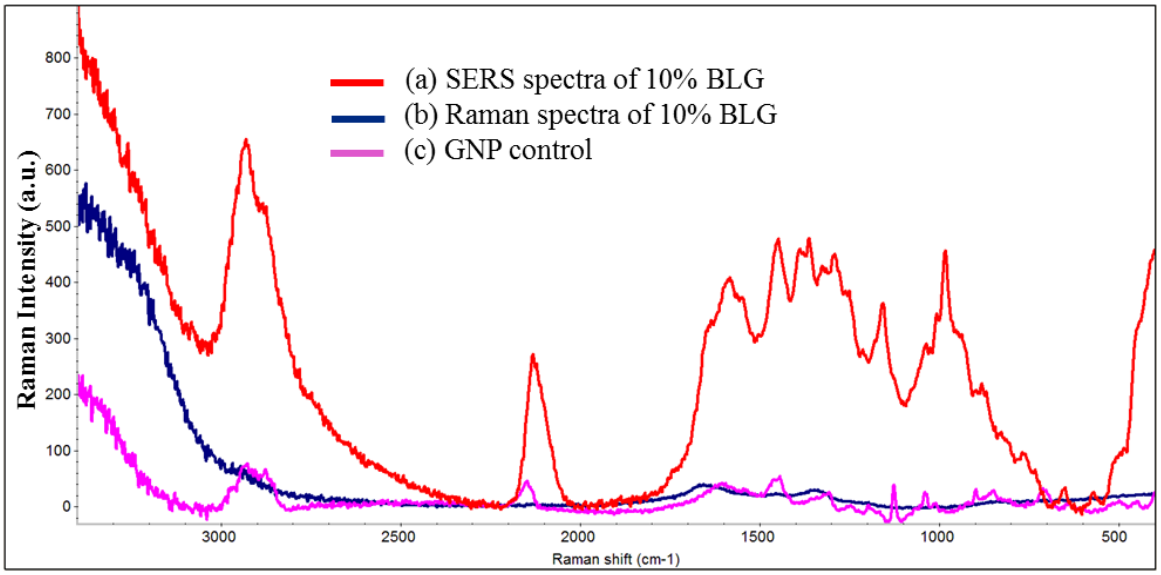

Figure 18: (a) SERS spectra of 1% BLG solution. (b) Raman spectra of 1% BLG solution. (c) GNP control.

As can be seen from the two BLG solutions, the lower concentration has a higher intensity. This can be attributed to the proximity to the GNPs. With the higher concentration of the 10% solution, there is more material masking the GNPs and limiting

the enhancement. This masking effect is also taken into account when doing experiments with oil.

Since the BLG was able to be enhanced, the amphiphilic GNPs were applied to an emulsion. The BLG in the emulsion was no able to be detected with normal Raman. But after introducing the amphiphilic GNPs to the emulsions there was a minor increase in the peak at 1350 cm-1 which is representative of the BLG peak and no other constituents.

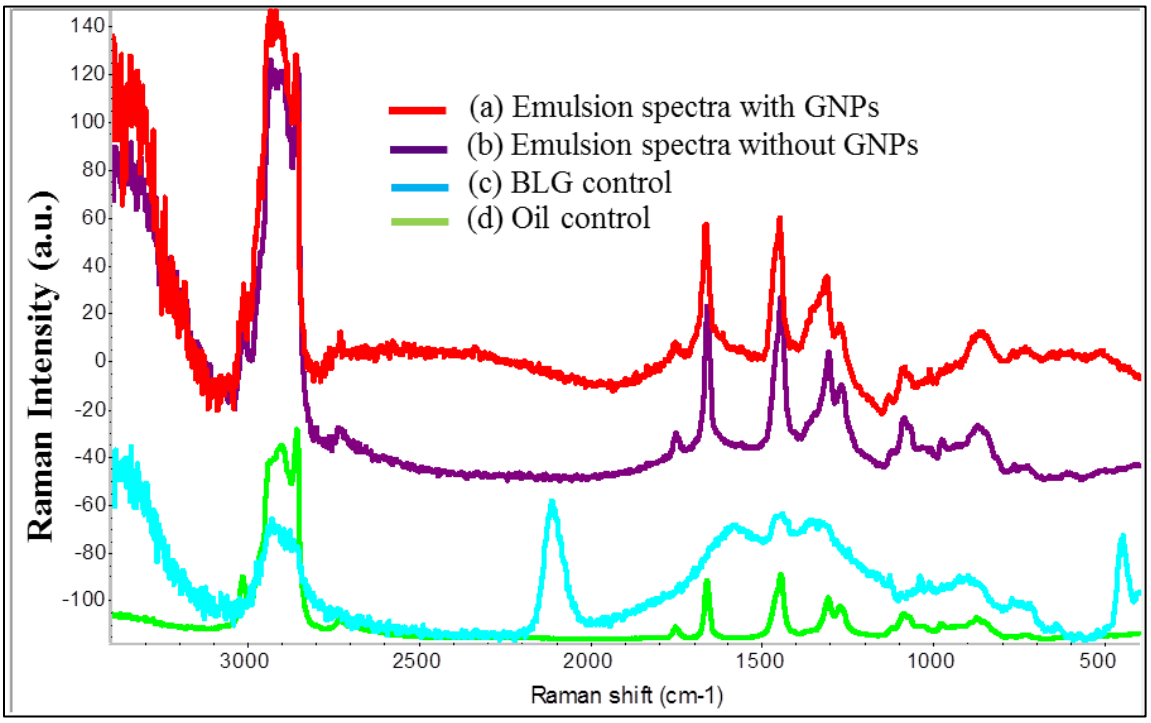

Figure 19: Raman spectra of amphiliphic GNPs, BLG, an emulsion control and an emulsion with the amphiliphic GNPs. There is a slight increase in the peak at 1350 cm-1 which is representative of BLG.

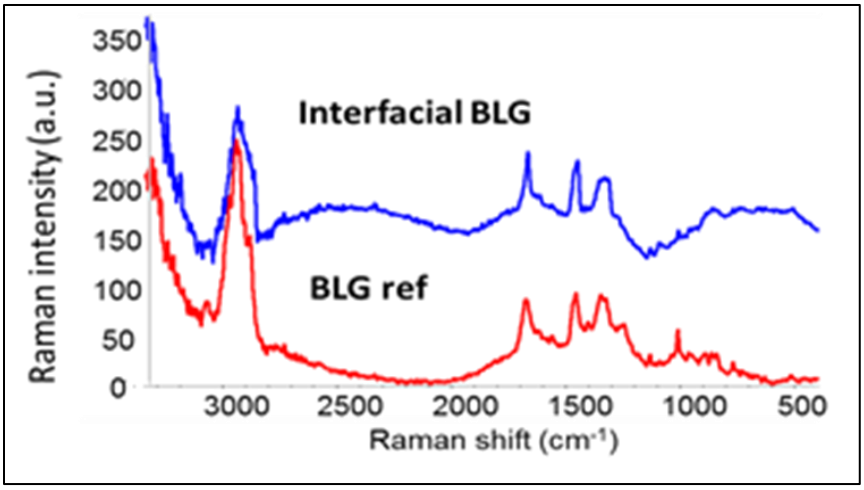

Figure 20: The interfacial properties can be determined with the addition of amphiphilic GNPs. There are characteristic peak changes compared to the control that can be seen only in the sample with modified GNPs.

The enhanced signals were thought to be mainly from the molecules adsorbed onto the surface of GNPs. Compared with the references which were recorded using solid powder (BLG) under the normal Raman parameters (without the use of GNPs, and a laser power at 24 mW) the extracted interfacial SERS spectra showed great enhancement and also spectral differences. The spectral difference can be attributed to a conformational change of the BLG after being emulsified and adsorbed onto the GNP surface. The stability of the emulsion was the same as the one without GNPs.

4.4. Detection of lipid oxidation products using conventional techniques

Three traditional lipid oxidation techniques were used to monitor lipid oxidation as a standard for the SERS method. Because conjugated dienes and peroxides are primary products of lipid oxidation, it was expected that their values increase with time. Hexanal is a secondary product so it takes more time to develop, which may be longer than this experiment.

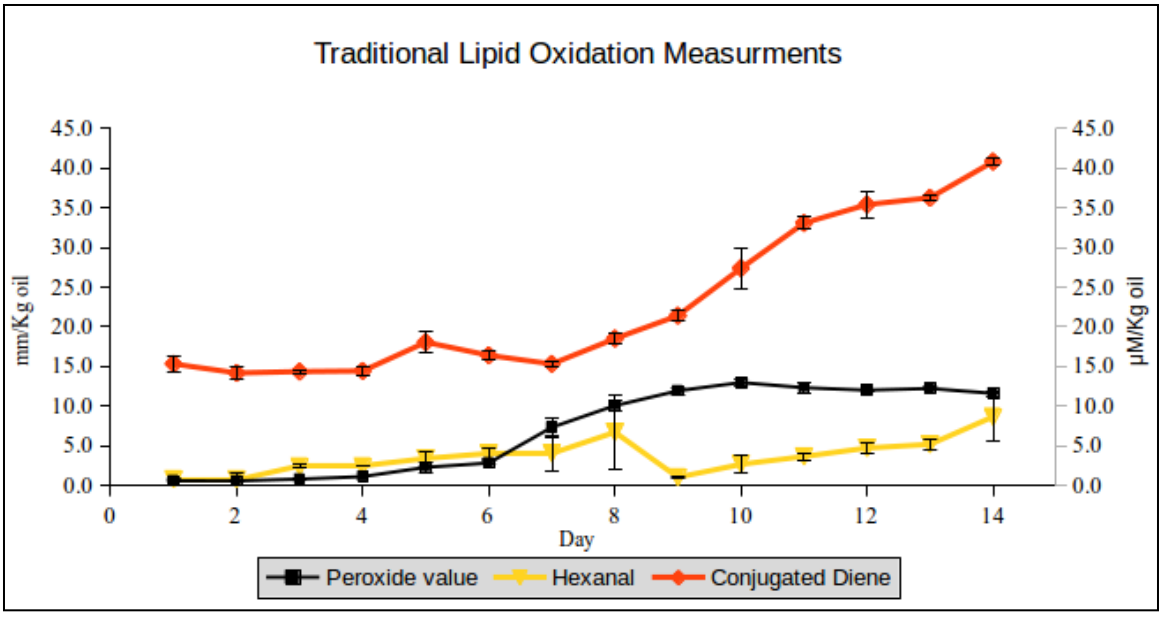

Figure 21: Conjugated Dienes, peroxide values and hexanal values of canola oil increase over time.

4.5. Detection of lipid oxidation products using normal Raman based TPP Chemical methods

TPP is capable of oxidizing when in contact with peroxides. TPP and TPPO were determined to have a differing spectra from one another based on peak heights and peak shifts.

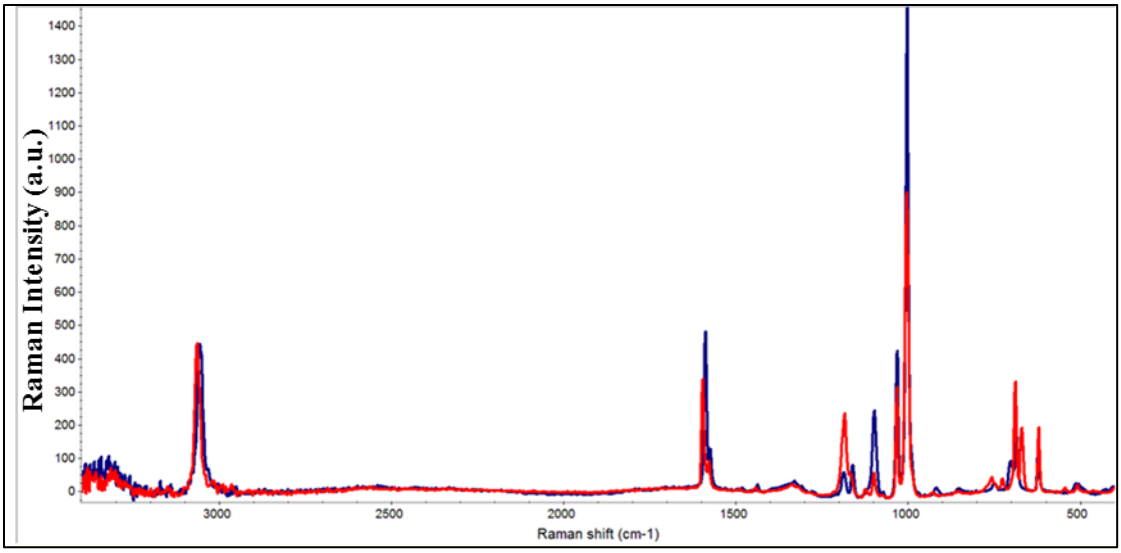

Figure 22: Raman spectra of TPP (blue) and TPPO (red). There are minor variations, including Raman shifts at 3100 and 1700 and peak intensity differences at 1000 and 800.

When applying this method to canola oil, the signals from the TPP are very small it is important to view the data in a proper way. The first way to observe the data is just by the full spectra. Using this view changes are visible, but difficult to differentiate and validate. Using the second derivative, changes become easier to differentiate. When zooming in on a particular band, it was found that at 705cm-1 had a positive trend in relation to peroxide value. As TPPO increases, the peak at 705cm-1 increases. In figure # there is a correlation between the peroxide value using the traditional spectroscopic technique and the amount of TPPO in the system measured by Raman.

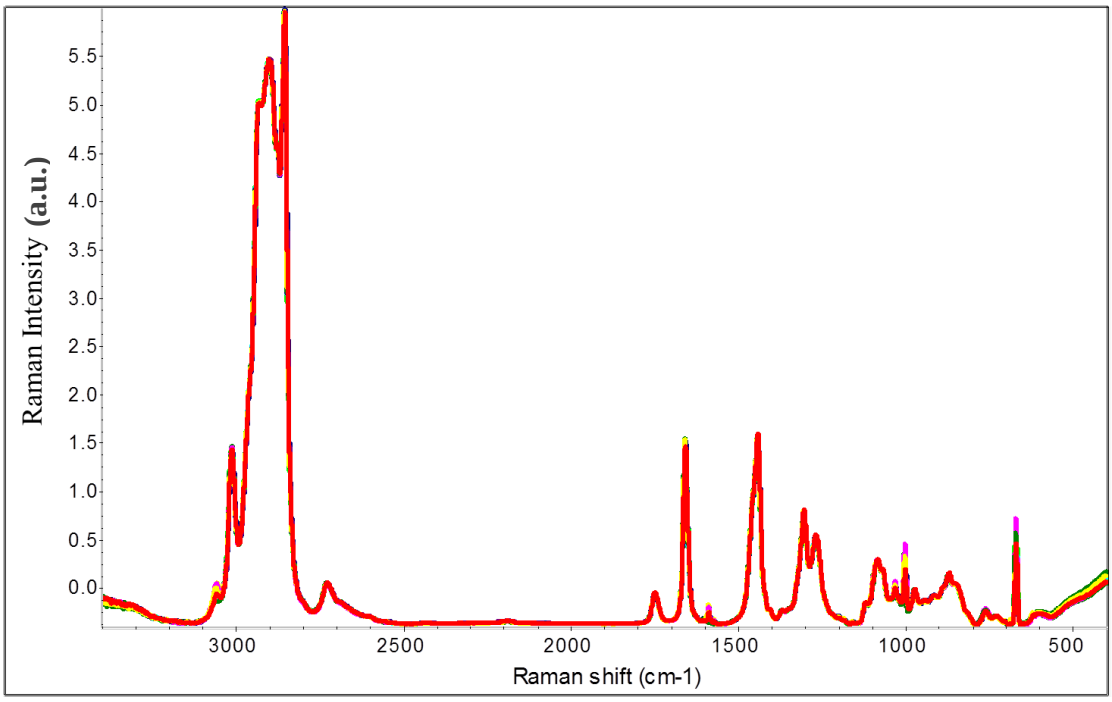

Figure 23: Raman spectra of canola oil from day 0 to day 14 with added TPP. When viewing the whole spectra, no trend is evident.

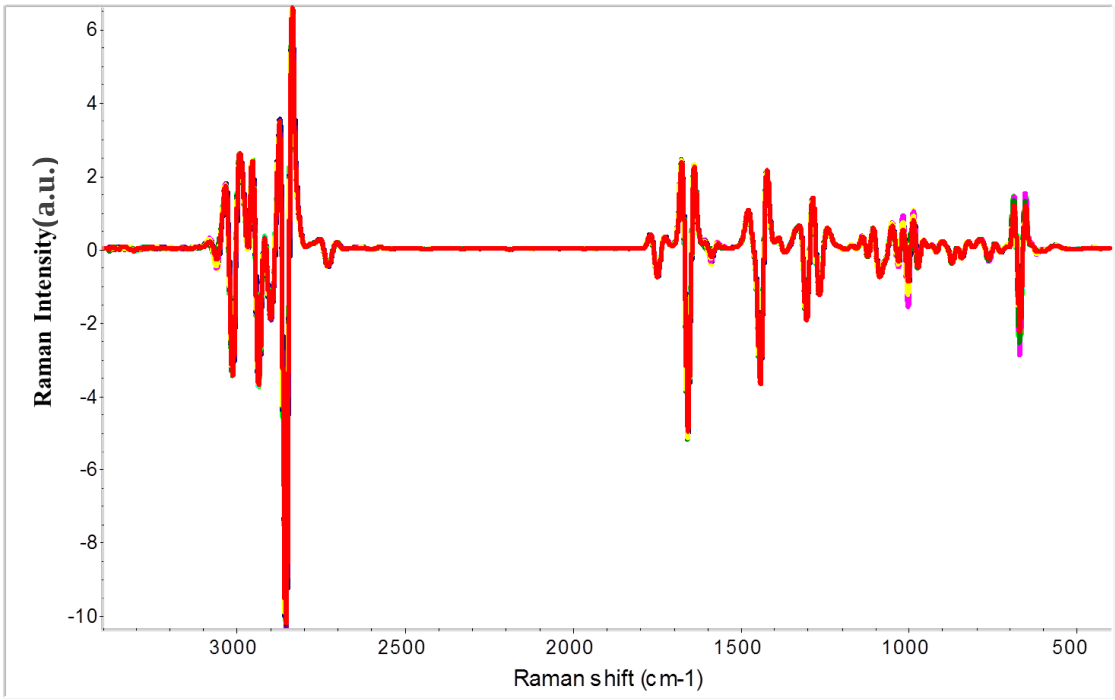

Figure 24: 2nd derivative of the Raman spectra of canola oil at day 0 and day 14 with no evident trend.

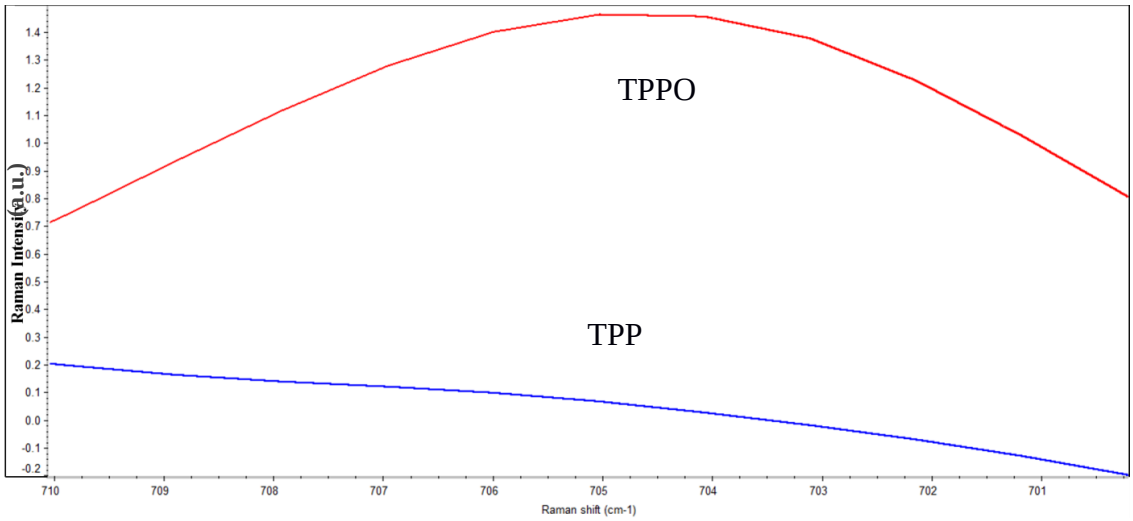

Figure 25: Zoomed in of the TPP and TPPO Raman spectra at 705 cm-1 where there is a major intensity difference.

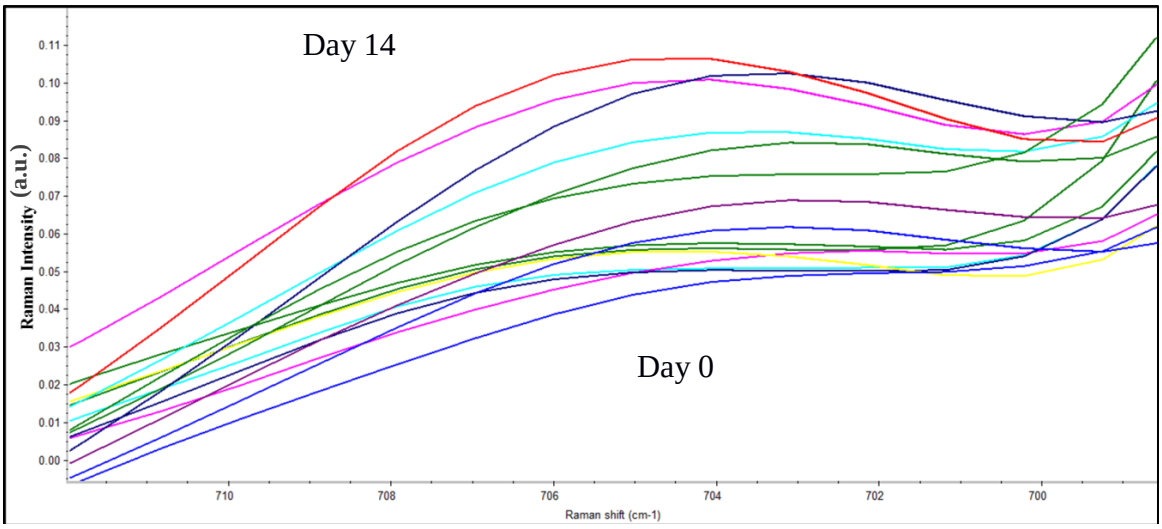

Figure 26: Zoomed in at 705 cm-1 for canola oil at day 0 and day 14 where there is a linear trend.

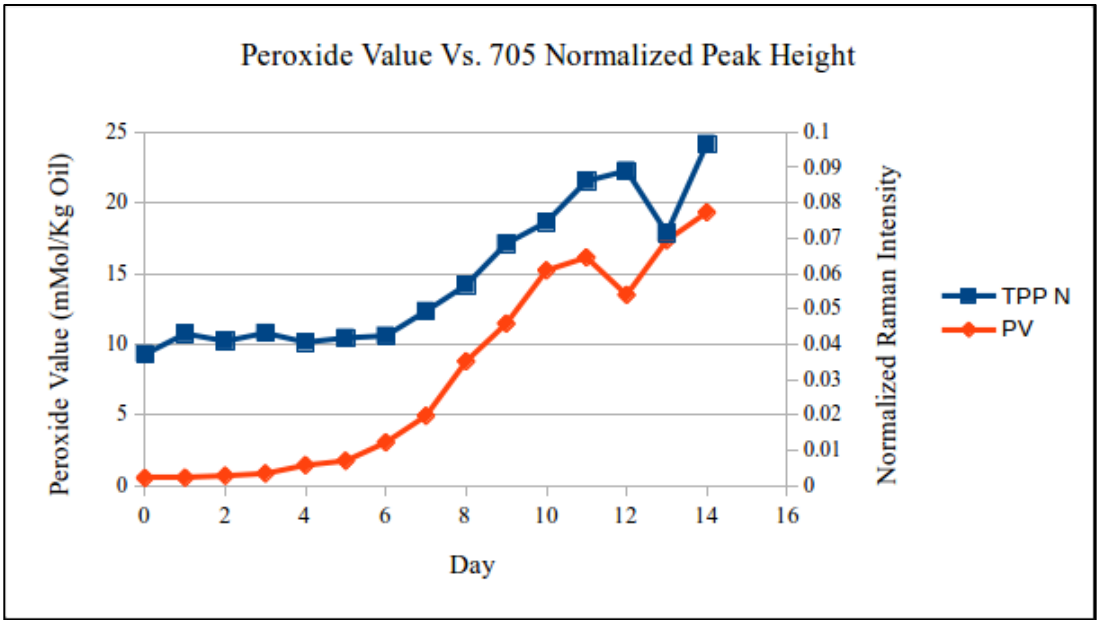

Figure 27: Graph of the normalized intensity values of canola oil with added TPP over 14 days compared to the PV values of canola oil using the traditional method.

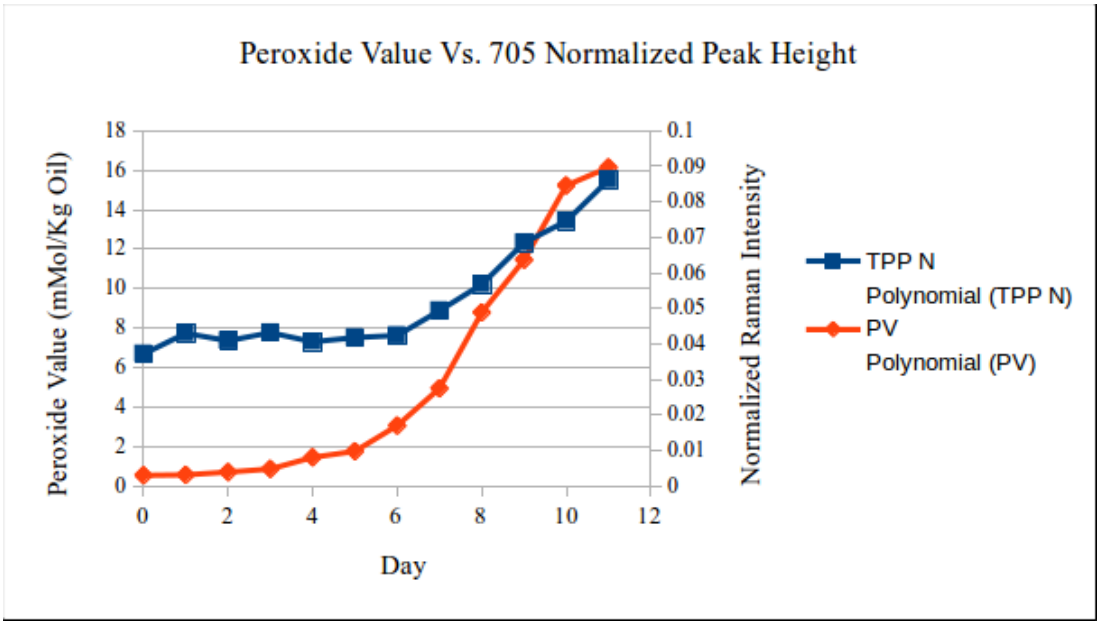

Figure 28: Graph of oil with TPP and PV values over 11 days, negating the outlier at day 12 and 13. The trend is very strong and values can be extrapolated from the TPP method.

TPP: f(x) = 0.2013182611x^2 – 0.0031995504x + 0.8861112976, r^2 = 0.983
PV : f(x) = 0.0006442058x^2 – 0.0031995504x + 0.0424835165. r^2 = 0.966

4.6. Enhancing lipid signals using hydrophobic GNPs

After producing the hydrophobic GNPs, they were applied to canola oil. As previously mentioned, it is possible to mask the gold nanoparticles and enhancement with the material being tested, so a proper dilution is important. To minimize the masking, the procedure used diluted the oil to 3%. The low dilution has a minimal normal Raman signal, which is also beneficial in measuring the enhancement factor. When preparing the SERS sample, the oil was diluted to 3%, but using the GNPs dispersed in hexane.

The first trial of canola oil oxidation used the hydrophobic GNPs which were not purified. The trial lasted from day 0 to day 7 taking both normal Raman measurements and SERS measurements of t 3% canola oil. Visually, there were no differences between the normal Raman signals from day 0 and day 7. The SERS signals did show some change, but the peaks simply decreased throughout the spectra. Using the PCA scores, there was no statistical difference between the normal Raman signals. But, there was a statistical difference between the two SERS signals. Although they were statistically significant, the resolution was low which lead to further investigation.

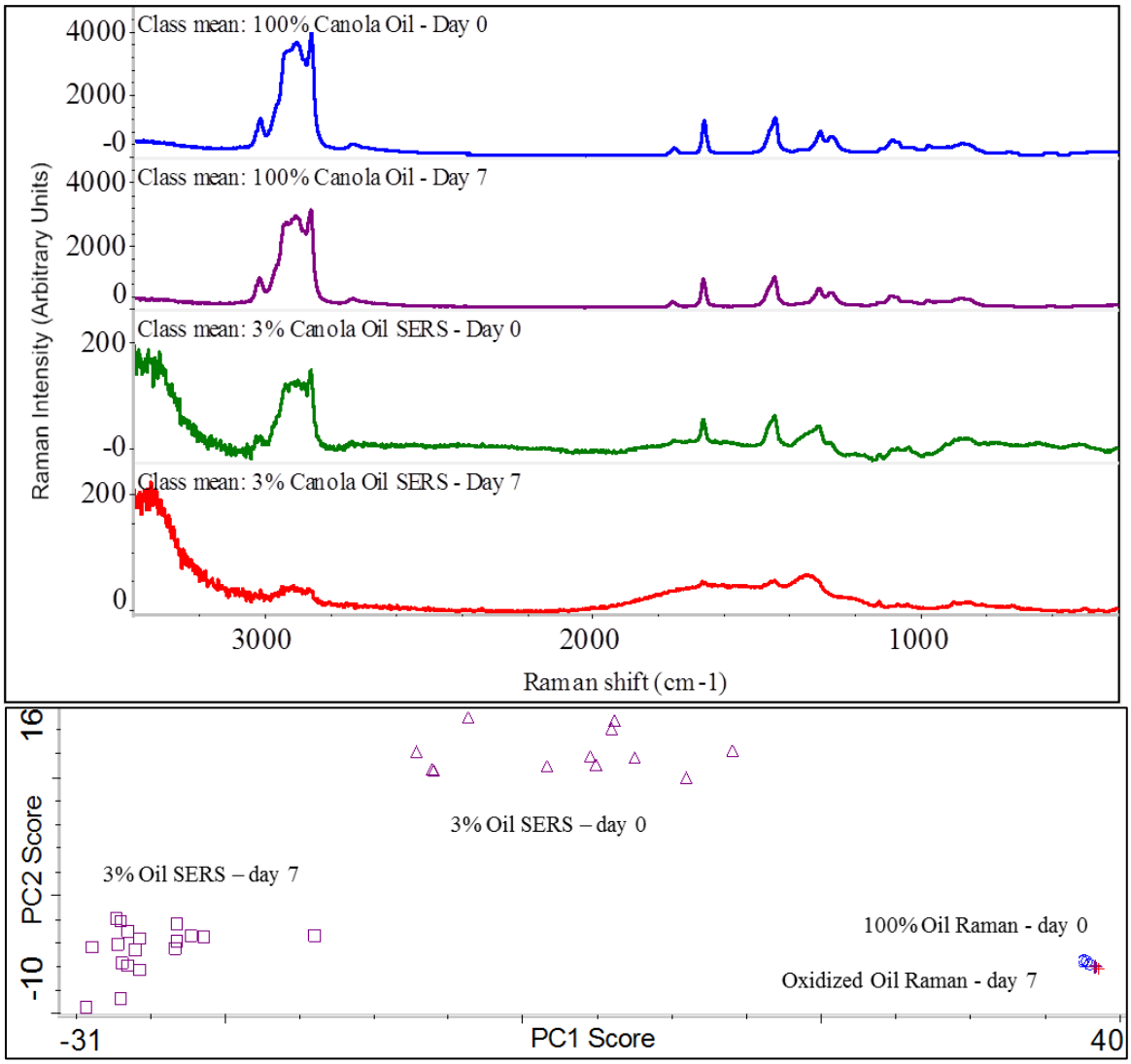

Figure 29: Raman signals of oil compared to SERS signals of oil over 7 days. (A) Under normal Raman, there was no change in pure canola oil after 7 days of 37^{o} C. Using the non-purified hydrophobic GNPs, there was a statistical change as seen in (B), in the diluted oil, although the resolution was low.

After observing the results of the previous experiment, purified GNPs were created and used to optimize the enhancement of the oil. When compared to the unpurified GNPs, the enhancement factor is higher and the resolution is better.

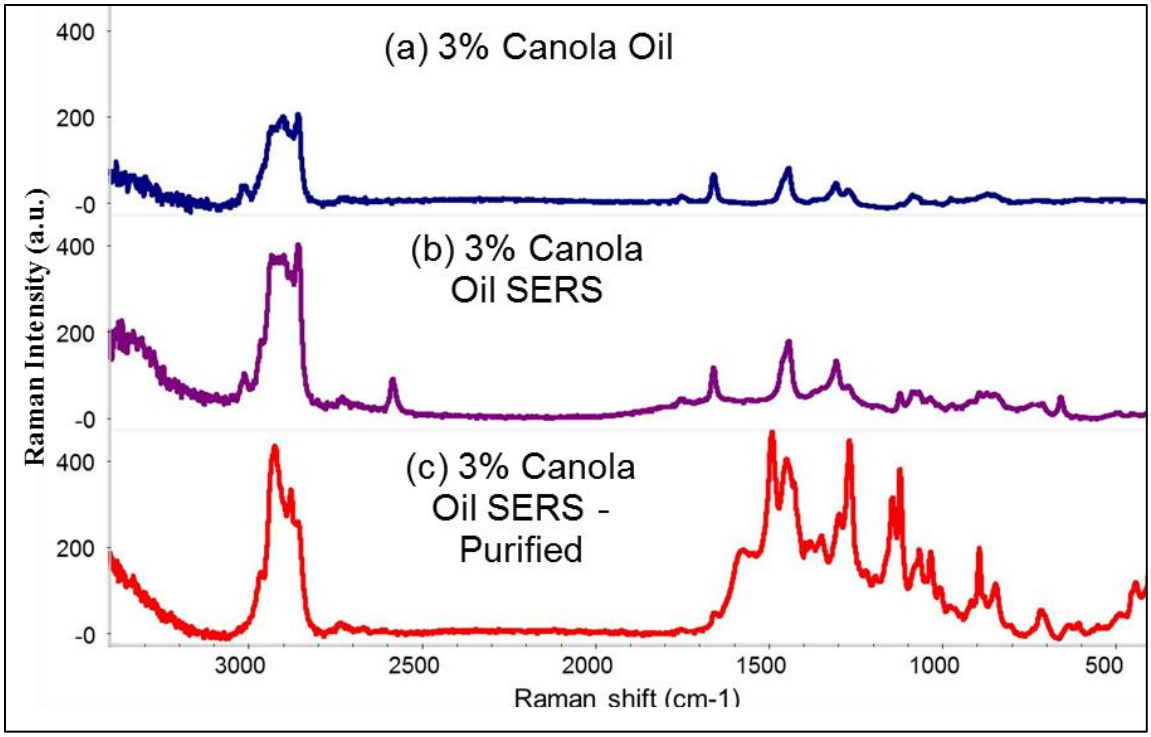

Figure 30: The effect of hydrophobic GNPs on diluted canola oil. (a) is normal Raman. (b) is non-purified GNPs with 3% canola oil. (c) is purified GNPs with 3% canola oil. The purification greatly increases the resolution of the Raman signals.

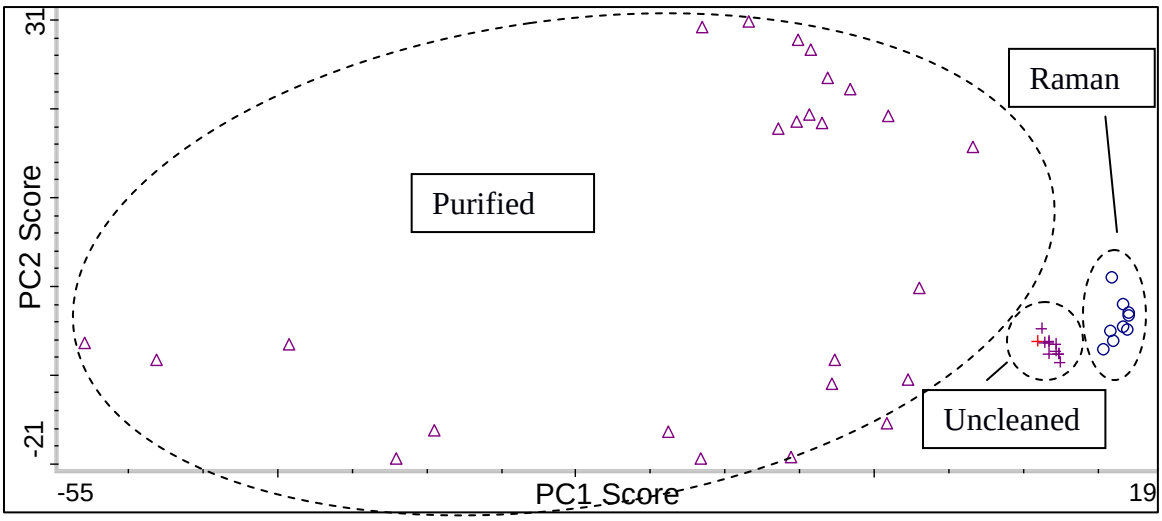

Figure 31: PCA scores of purified hydrophobic GNPs with canola oil after normalization.

The purified GNPs were applied to canola oil at day 0 and day 7 to monitor changes. There were clear visual changes over time, and some of which can be characterized, primarily a change in –CH2 and =C-H.

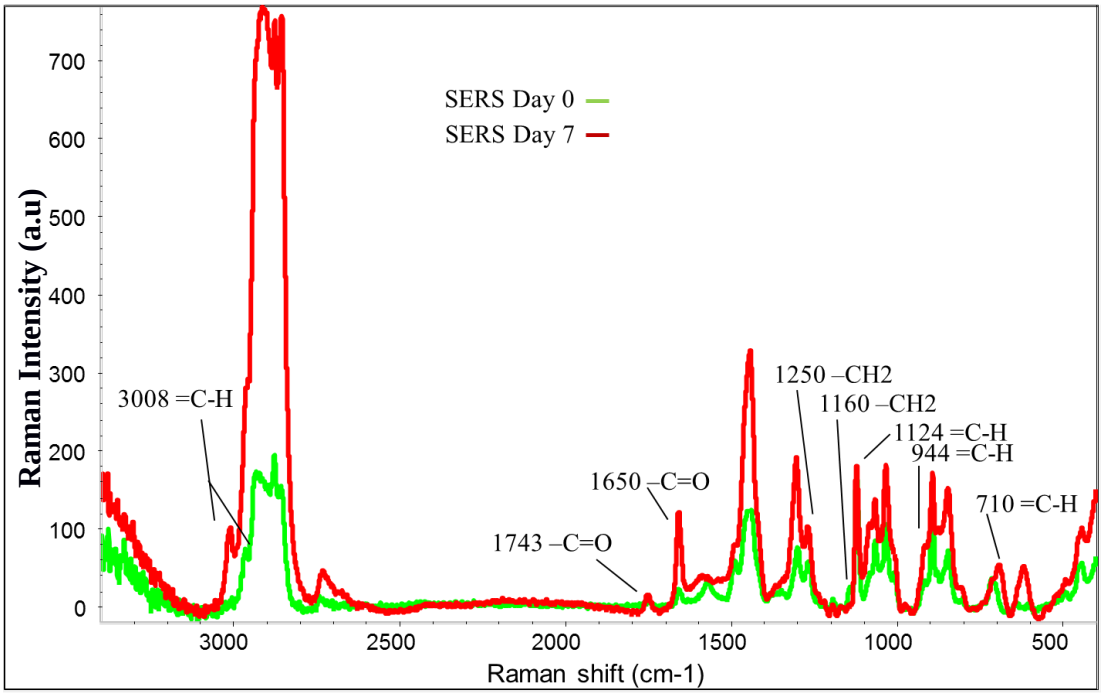

Figure 32: Hydrophobic GNPs with canola oil over 7 days. After purification, enhancement was more apparent.

Daily trials were started on day 0 through day 11, following the same format as the previous experiment. There was no major trend or marker than could be seen and used for oxidation, but there were changes in the spectra. One of the primary issues with this method is the variation within a sample. Because lipids are complex molecules and enhancement is a complicated phenomenon, signals vary greatly. As shown in figure 15, just one sample provides many different spectra. The data is shown in a number of ways including the raw spectra, the normalized spectra and the second derivative spectra. Each has their benefits of data analysis.

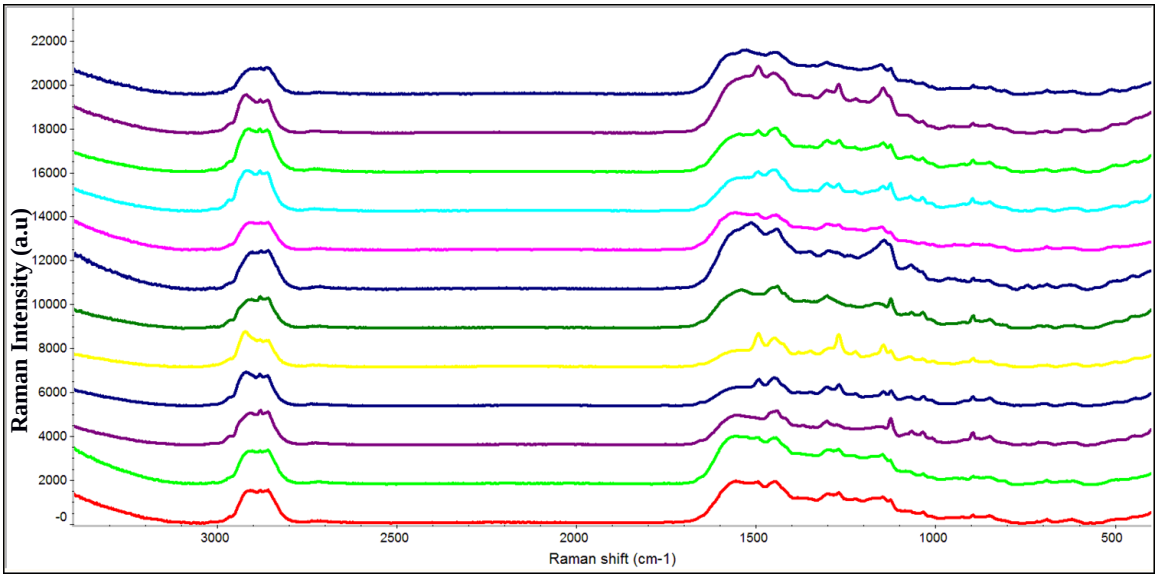

Figure 33: Canola oil and hydrophobic GNPs Day 0 to day 11 compared.

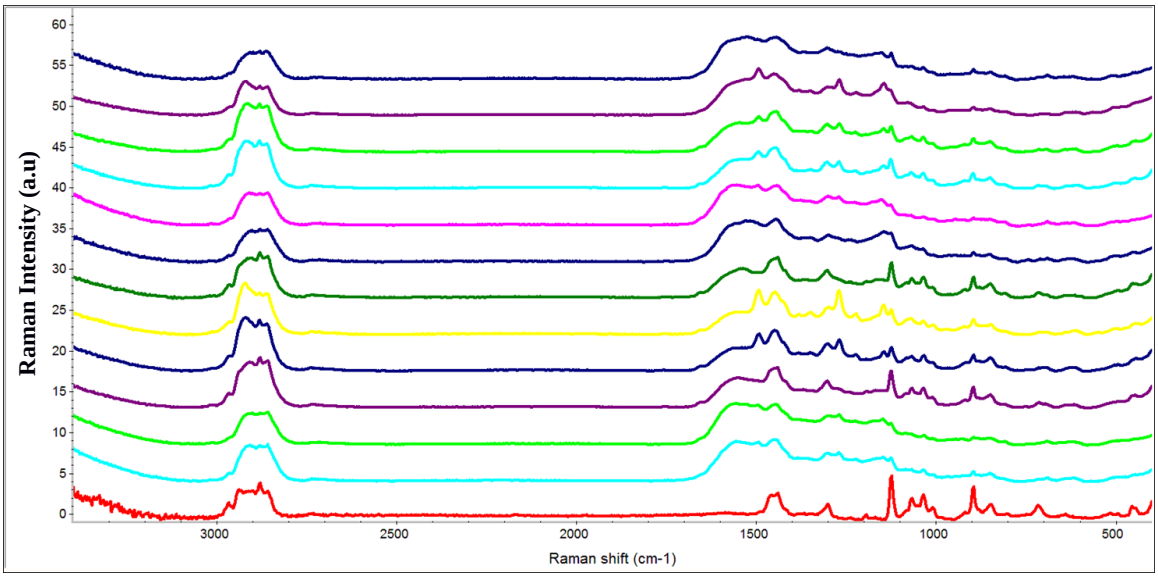

Figure 34: Canola oil and hydrophobic GNPs day 0 to day 11 normalized with the gold control.

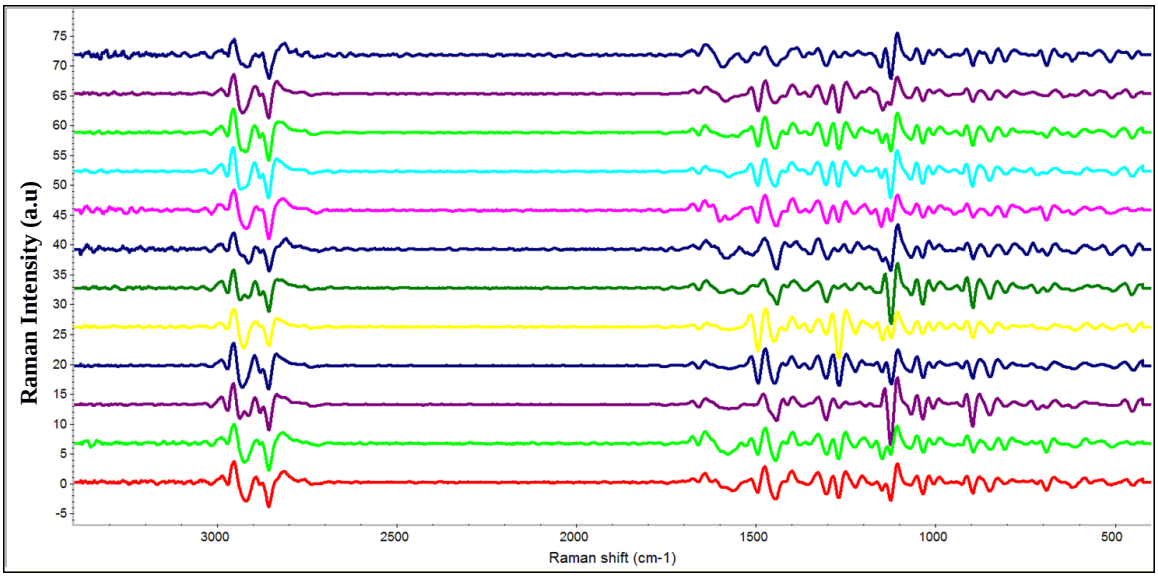

Figure 35: Canola oil and hydrophobic GNPs day 0 to day 11 in 2nd derivative format compared.

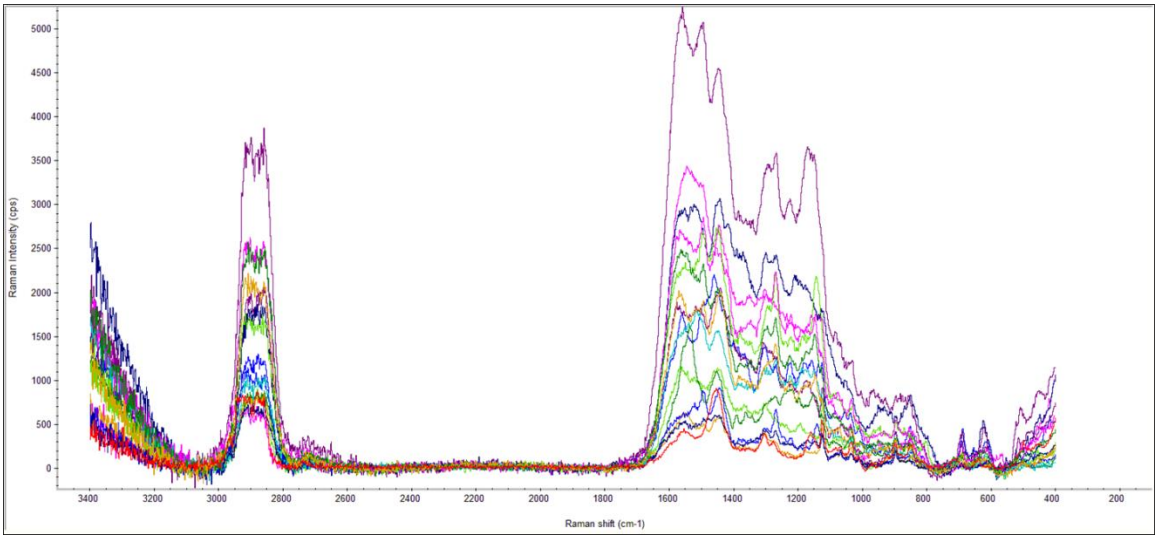

Figure 36: Variation among day 11 readings

4.7. Modified Steel wire for volatile analysis

Following the method for the modification of a steel wire, it was found to be possible to measure the modification using Raman. In figure (this) the steel wire and gold modified steel wire have distinctly different spectra.

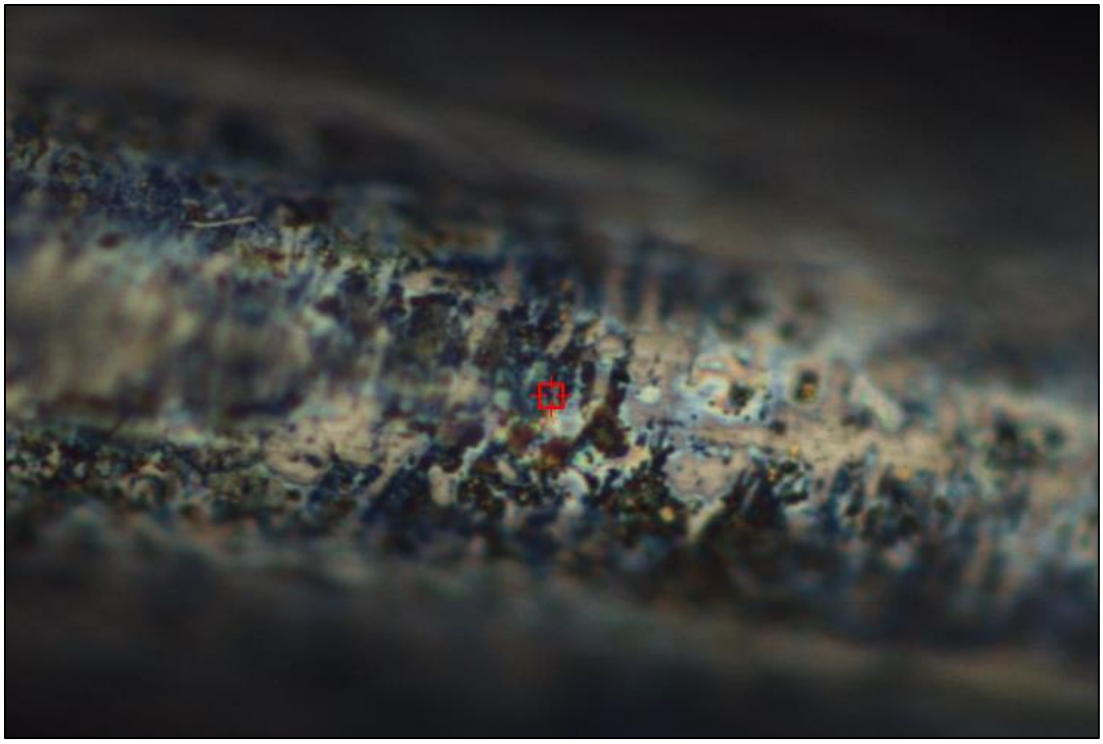

Figure 37: GNP modified stainless steel wire under optical microscope (50x).

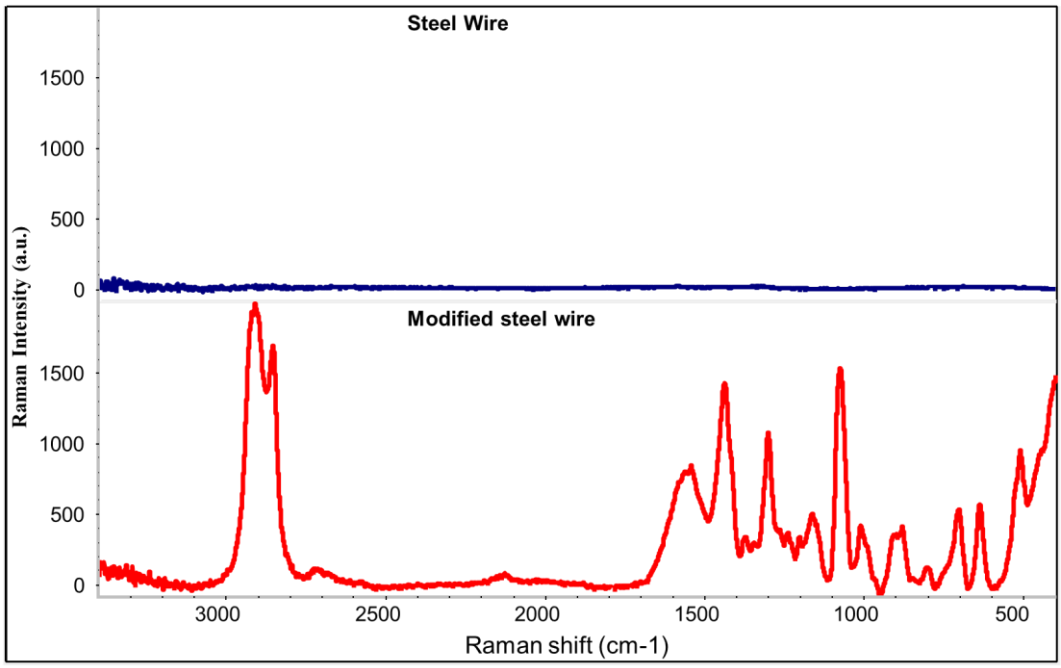

Figure 38: Raman spectra of the stainless steel wire and GNP modified SS wire

In order to test the viability of the headspace analysis, the modified steel wire was placed in a tube with one of two lipid oxidation control products. The results show that it is possible to enhance the volatile products, more so with the more hydrophilic ones.

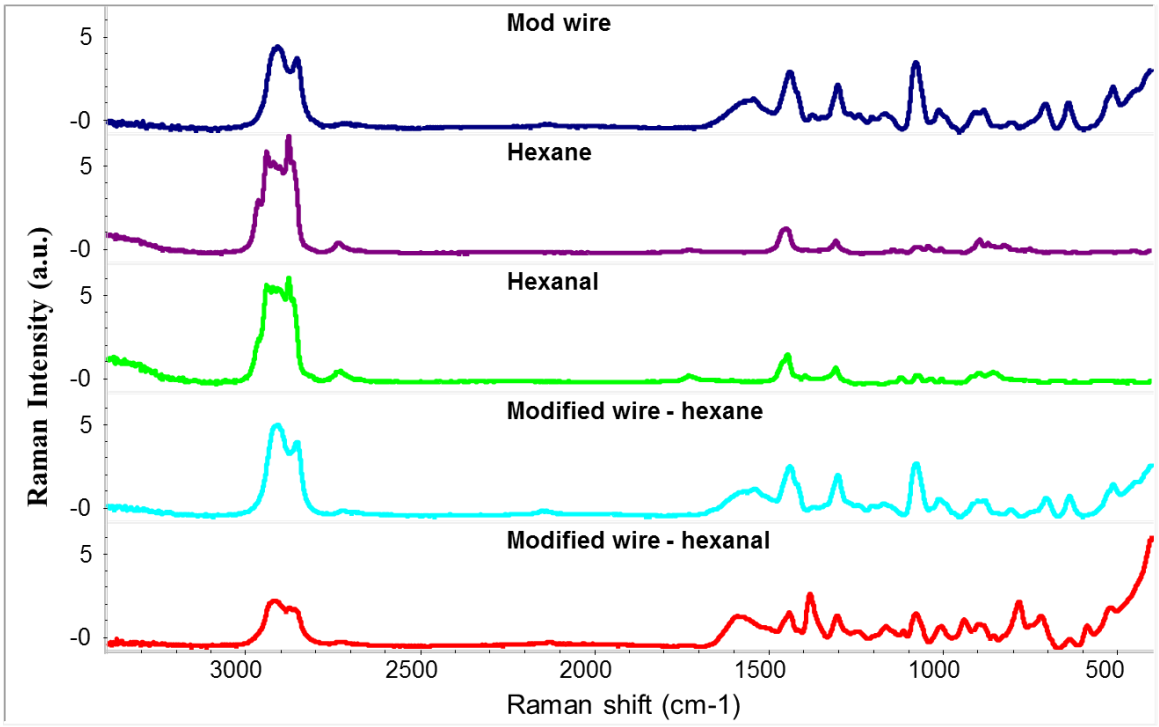

Figure 39: Modified steel wire with two lipid oxidation controls molecules

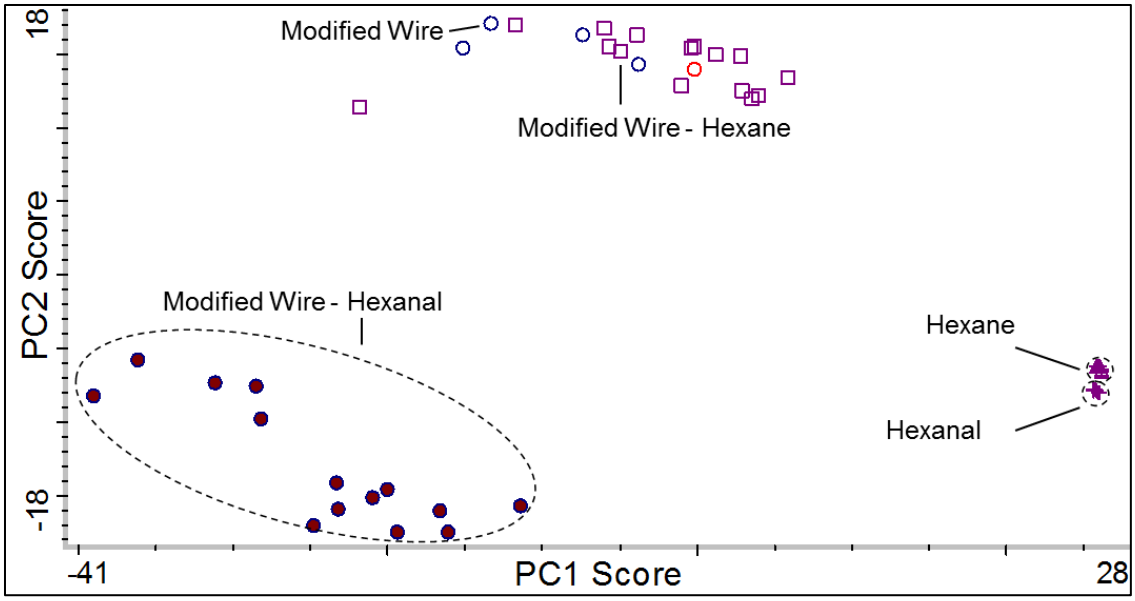

Figure 40: PCA plot of modified steel wire with two lipid oxidation controls.

Over two weeks, oils were measured using the modified steel wires. As seen with the other SERS results, enhancement is good, but consistency is not good due to high variability in a lipid system.

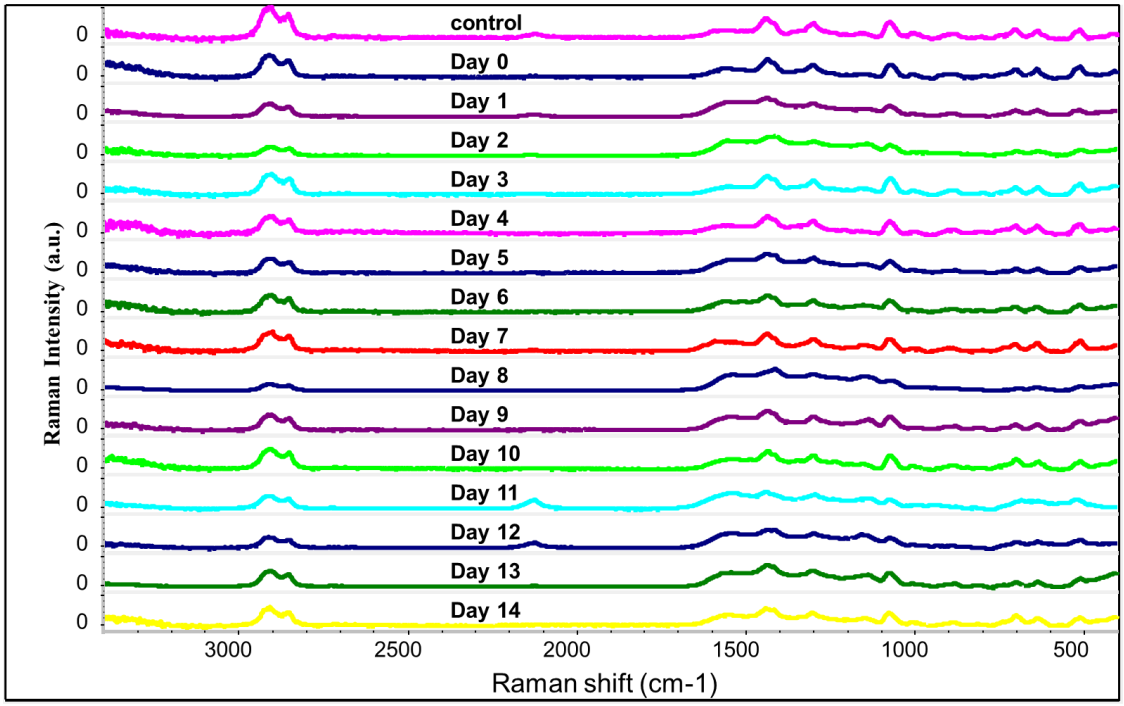

Figure 41: Raman spectra of the GNP modified SS wire in canola oil from day 0 to day 14 stacked.

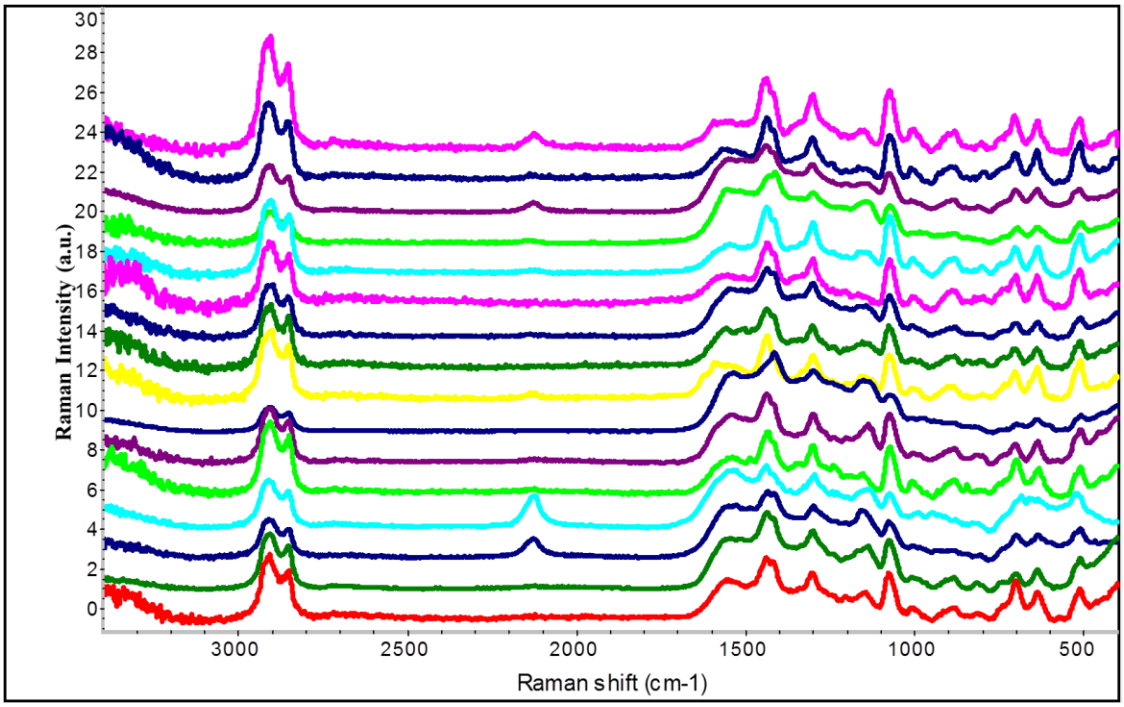

Figure 42: Raman spectra of the GNP modified SS wire in canola oil from day 0 to day 14 normalized.

4.8. Detection of lipid oxidation products using SERS with silver dendrites

Canola oil at 5% has a very weak signal under the 10x objective, but when placed on top of Ag dendrites, characteristic peaks appear, suggesting enhancement of the oil. The band at 2850 cm−1 represented the CH stretch. The band at 1665 cm−1 represented the C-C stretch. The band representing the CH3 and CH2 deformations were found at around 1450 cm−1. Interestingly, there was a new peak at 1616 cm−1 in the SERS spectra of canola oil that was neither in the normal Raman spectrum nor in the silver control spectrum. In addition, not all the samples had this peak. The appearance of this peak was found in about 50% of the tested samples. The origin of this new peak was not clear. It may be the result of a random interaction between the lipid molecules and Ag surface where a unique structure of the lipid molecules was enhanced.

Under normal Raman, 100% canola oil presented no visual or statistical difference between day 0 and day 30. Using the SERS techniques, a significant different occurred at day 5 according to PCA analysis. The decrease of the major lipid peaks from 2950 to 2850, 1665, and 1450 cm−1 may be due to the loss of the reactant. However, not only the lipid peaks decreased, the silver background peak (i.e.NO_3 peak at 1075 cm−1) was also found to decrease, at an even higher rate than the lipid peaks. As discussed previously, the NO_3 peak is an indicator of the other molecules on the Ag dendrites. The decrease of the NO_3 peak indicates the increase of total molecules on the Ag dendrites. The increased molecules here were believed to be the secondary oxidation products, e.g. alcohols, saturated aldehydes,α,β-unsaturated aldehydes and epoxy compounds. When the number of secondary product molecules that were over the surface of Ag dendrites reached the maximum amount that the Ag could enhance, the overall peak intensity would drop due

to the masking effect. To prove the speculation, we further diluted the oil at day 30 to 0.1%. Compared to 1% oxidized canola oil, the overall peak intensity of 0.1%oil increased, including the silver back- ground peak at 1075 cm−1. This result confirmed that the over- all analyte molecules increased after the oxidation of the oil. As seen in Fig. 2, the relative peak intensity of 0.1% canola oil (before oxidation) was much lower as compared to 1% canola oil, while after oxidation, the production of secondary oxidation products resulted in the increase of total analytes, leading to the higher peak intensity at 0.1% concentration. The spectrum of diluted oxidized oil showed more variance than the oil at day 0. Peak shift and new peaks were observed. For example, the noticeably increased peak at around 1777 cm−1 may be due to the C-O stretching of the aldehydes. The 1657 cm−1 peak was found to be shifted to 1633 cm−1; a possible explanation was due to the formation of trans and conjugated double bonds. More systematic experiments are needed to elucidate the mechanisms of spectral changes resulting from lipid oxidation.

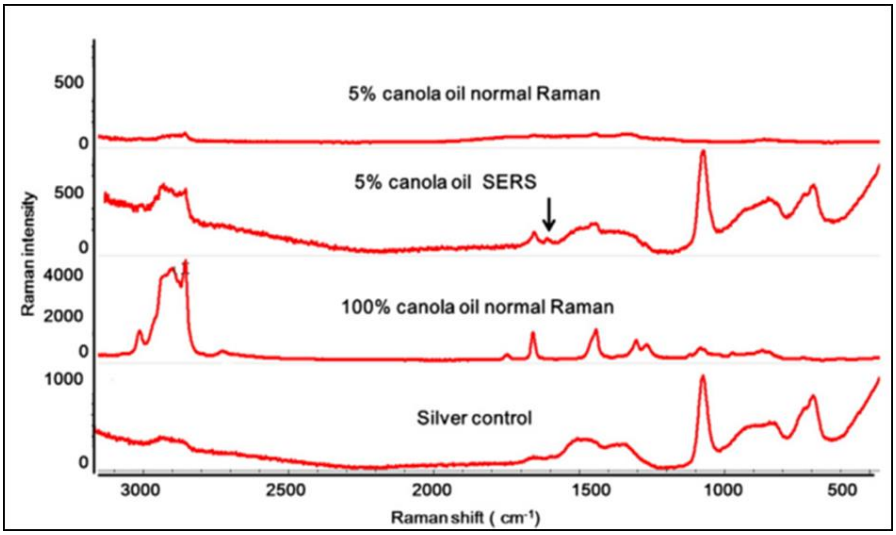

Figure 43: Raman and SERS spectra of 5% canola oil, 100% canola oil control and silver dendrite control.

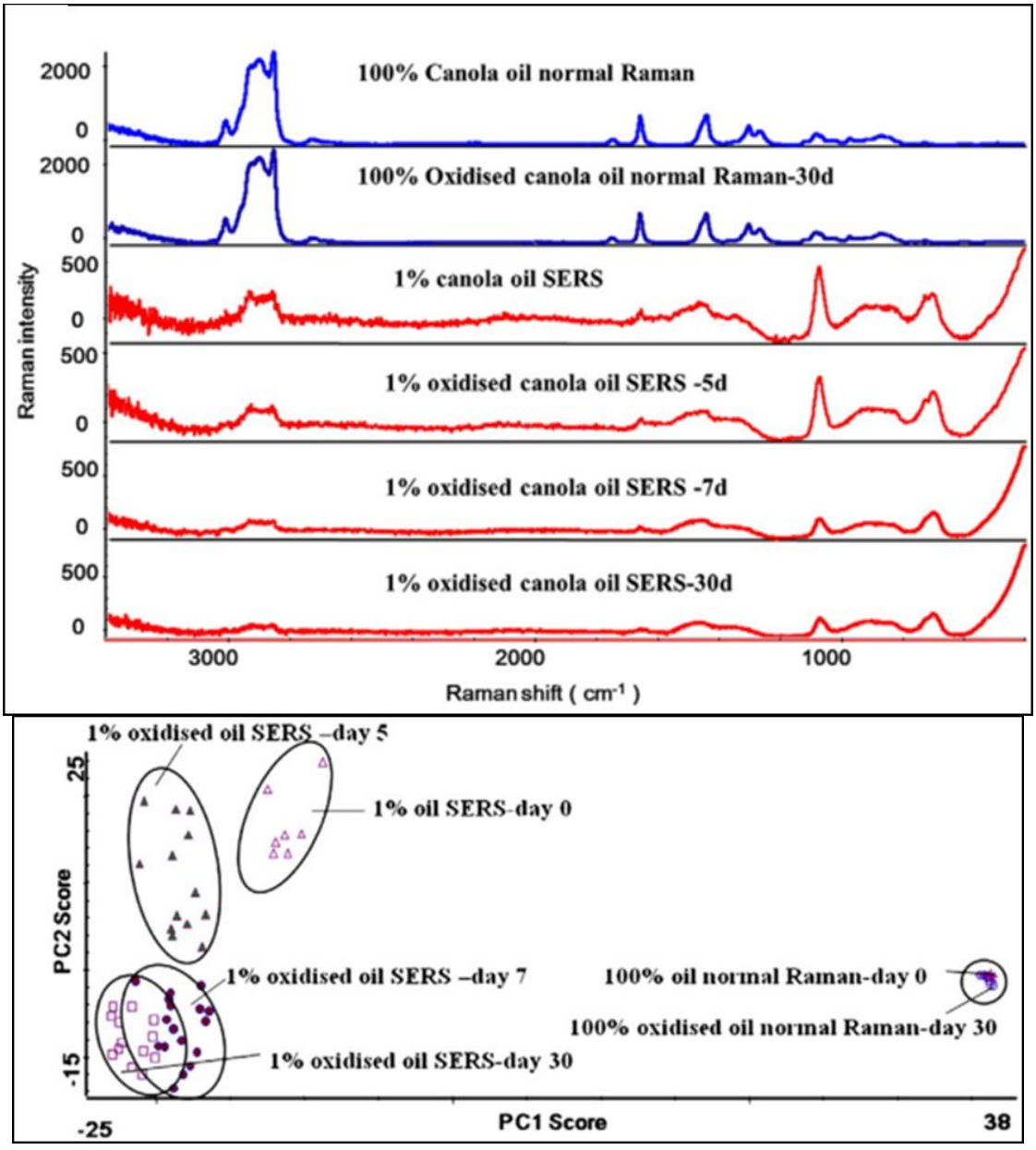

Figure 44: Canola oil on silver dendrites over time and PCA scores.

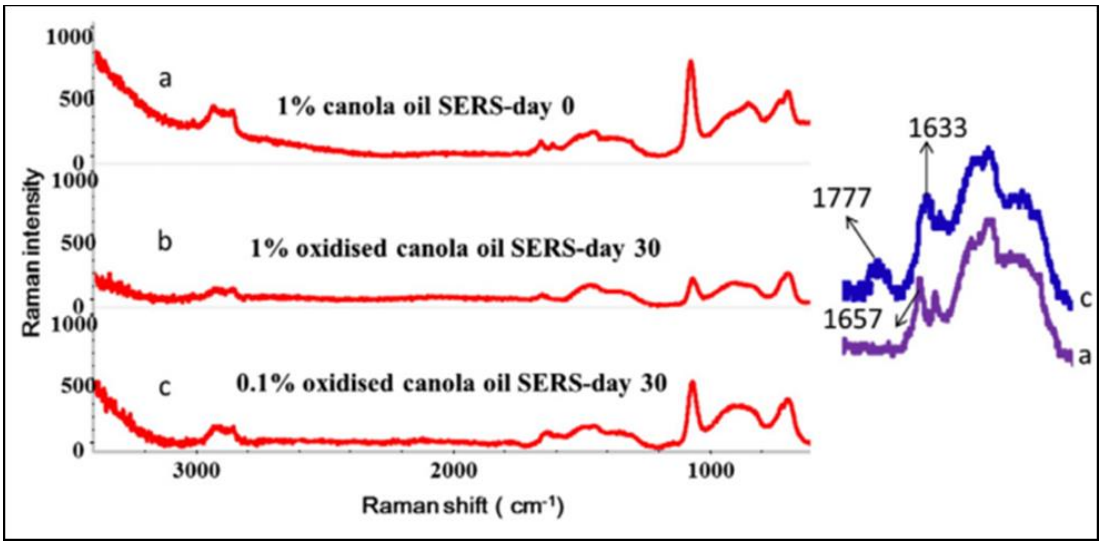

Figure 45: Canola oil on silver dentrides and peak changes over 30 days.

4.9. Enhancing lipid signals using the sandwich method

Utilizing two SERS substrates, the sandwich method provides a higher consistency among SERS spectra. The one major issue with this method is the background peak from the silver dendrites from the nitrate. The addition of the gold did not provide a higher enhancement for the canola oil, but the consistency was slightly improved. When the GNPs were used alone, the Raman intensity varied up to 4000 a.u. Using the sandwich method, the peak intensities were more consistent; within 1000 a.u.

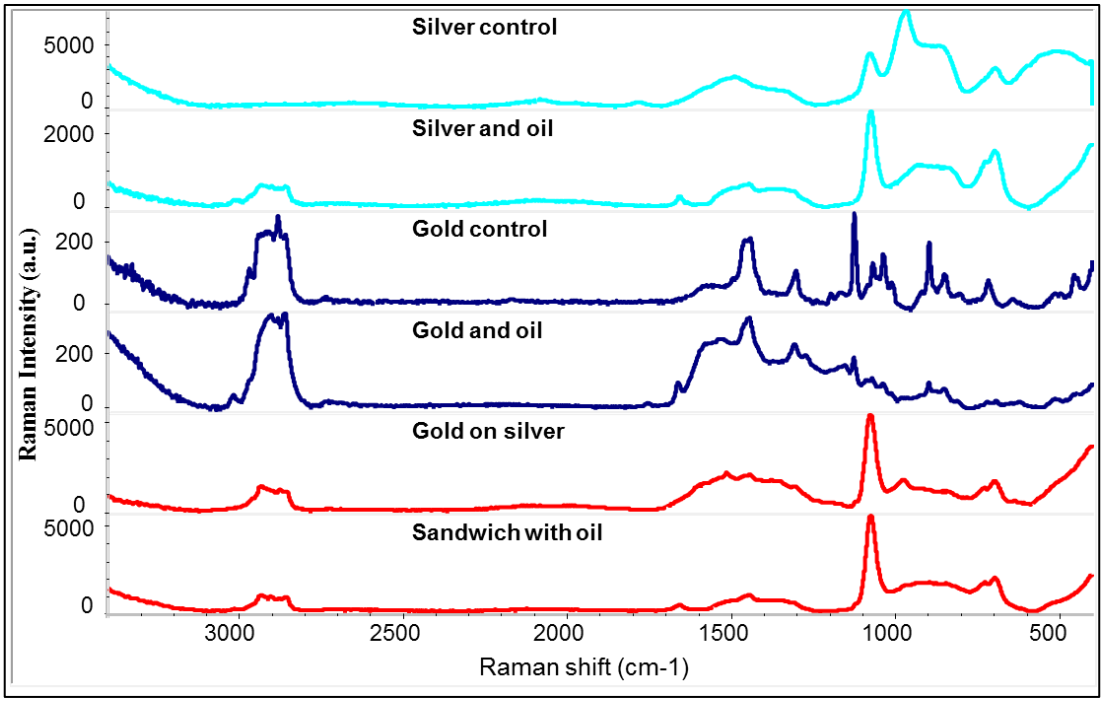

Figure 46: Raman spectra the controls and test samples for the sandwich method

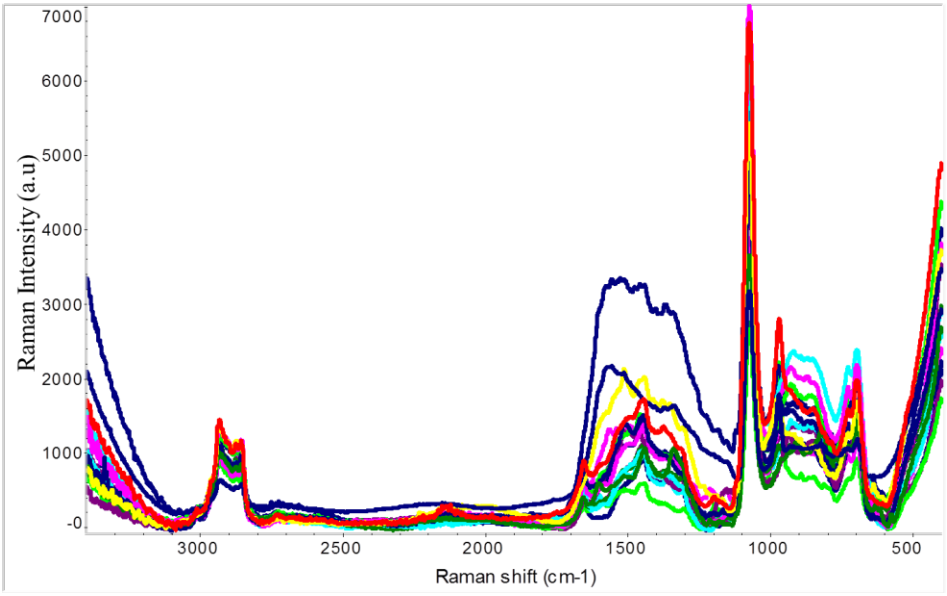

Figure 47: Raman spectra of canola oil with the sandwich method from day 0 to day 14 overlayed.

4.10. Summary of methods

Method	Results	Problem
Hydrophobic GNPs	Good enhancement	High variation
TPP	Good peroxide correlation	Only measures peroxides
Modified steel wire	Good enhancement	High variation, difficult preparation
Silver dendrites	Moderate enhancement	Low resolution
Sandwich	Moderate enhancement	Low resolution

Table 2: Summary of SERS enhancement method.

CHAPTER 5

SUMMARY AND CONCLUSIONS

The chemical reaction of TPP to TPPO was quite successful in predicting the peroxide value of oil. At peak 705, there was a linear trend of intensity compared to actual peroxide value.

Based on the Raman data, colloidal GNPs are able to be modified using octanethiol, altering the hydrophobicity. The modification used different solvents and mixing methods to result in either amphiphilic GNPs or hydrophobic GNPs. The amphiliphic GNPs were applied to an emulsion to enhance the interfacial layer *in situ* and was capable of enhancing a characteristic peak of the emulsifier.

The hydrophobic GNPs were applied to canola oil to enhance the Raman signal and monitor lipid oxidation. The GNPs successfully enhanced the canola oil signals, but the variation among each day lead to inconsistent data and no major trend throughout oxidation.

Silver dendrites were capable of enhancing the Raman signal, but with low resolution. This was coupled with hydrophobic GNPs in the sandwich method for higher enhancement, but the resolution and enhancement was still low.

With these novel methods of lipid analysis with Raman and SERS, it opens the door for a more rapid and sensitive measurement of lipid oxidation. Although the methods require some revision for higher resolution and consistency, they have proved the capabilities of using Raman with food oils.

BIBLIOGRAPHY

Anker, J. N., Hall, W. P., Lyandres, O., Shah, N. C., Zhao, J., & Van Duyne, R. P. (2008). Biosensing with plasmonic nanosensors. *Nature Materials*, *7*(6), 442–453. Retrieved from http://www.nature.com/nmat/journal/v7/n6/abs/nmat2162.html

Anker, J. N., Hall, W. P., Lyandres, O., Shah, N. C., Zhao, J., & Van Duyne, R. P. (2008). No Job Too Small. *Nature Materials*, *7*(6), 419.

Baeten, V., Fernández Pierna, J. A., Dardenne, P., Meurens, M., García-González, D. L., & Aparicio-Ruiz, R. (2005). Detection of the presence of hazelnut oil in olive oil by FT-raman and FT-MIR spectroscopy. *Journal of Agricultural and Food Chemistry*, *53*(16), 6201–6. doi:10.1021/jf050595n

Baeten, V., & Hourant, P. (1998). Oil and fat classification by FT-Raman spectroscopy. *Journal of Agricultural and Food Chemistry*, *8561*(97), 2638–2646. Retrieved from http://pubs.acs.org/doi/abs/10.1021/jf9707851

Brust, M., Walker, M., Bethell, D., Schiffrin, D. J., & Whyman, R. (1994). Synthesis of thiol-derivatised gold nanoparticles in a two-phase Liquid?Liquid system. *Journal of the Chemical Society, Chemical Communications*, (7), 801. doi:10.1039/c39940000801

Chua, W., Chapman, P., & Stachowiak, G. W. (2012). Surface-Enhanced Raman Spectroscopy of Tribochemically Formed Boundary Films of Refined and Unrefined Canola Oils. *Journal of the American Oil Chemists' Society*, *89*(10), 1793–1800. doi:10.1007/s11746-012-2075-1

Craig, A. P., Franca, A. S., & Irudayaraj, J. (2013). Surface-enhanced Raman spectroscopy applied to food safety. *Annual Review of Food Science and Technology*, *4*, 369–80. doi:10.1146/annurev-food-022811-101227

Damodaran, S., Parkin, K. L., & Fennema, O. R. (Eds.). (2007). *Fennema's Food Chemistry* (4th ed.). CRC Press.

Fendler, J. H. (2001). Chemical Self-assembly for Electronic Applications. *Chemistry of Materials*, *13*(10), 3196–3210. doi:10.1021/cm010165m

Feng, J., Sun, M., Liu, H., Li, J., Liu, X., & Jiang, S. (2010). Au nanoparticles as a novel coating for solid-phase microextraction. *Journal of Chromatography. A*, *1217*(52), 8079–86. doi:10.1016/j.chroma.2010.10.089

Fleischmann, M., Iiendra, P. J., & McQuillan, A. J. (1974). Raman Spectra of Pyridine Adsorbed at a Silver Electrode. *Chemical Physics Letters*, *26*(2), 163–166.

Frens, G. (1973). Controlled Nucleation for the Regulation of the Particle Size in Monodisperse Gold Suspensions. *Nature Physical Science*, *241*, 20–22.

Ghosh, P., Han, G., De, M., Kim, C., & Rotello, V. (2008). Gold nanoparticles in delivery applications☆. *Advanced Drug Delivery Reviews*, *60*(11), 1307–1315. doi:10.1016/j.addr.2008.03.016

Giersig, M., & Mulvaney, P. (1993). Preparation of ordered colloid monolayers by electrophoretic deposition. *Langmuir*, *9*(12), 3408–3413. Retrieved from http://pubs.acs.org/doi/abs/10.1021/la00036a014

Häkkinen, H. (2012). The gold–sulfur interface at the nanoscale. *Nature Chemistry*, *4*(6), 443–455. doi:10.1038/nchem.1352

Haynes, C. L., McFarland, A. D., & Duyne, R. P. Van. (2005). Surface-enhanced Raman spectroscopy. *Analytical Chemistry*, *77*(17), 338–A. Retrieved from http://pubs.acs.org/doi/pdf/10.1021/ac053456d

He, L., Haynes, C. L., Diez-Gonzalez, F., & Labuza, T. P. (2011). Rapid detection of a foreign protein in milk using IMS-SERS. *Journal of Raman Spectroscopy*, *42*(6), 1428–1434. doi:10.1002/jrs.2880

He, L., Lin, M., Li, H., & Kim, N.-J. (2009). Surface-enhanced Raman spectroscopy coupled with dendritic silver nanosubstrate for detection of restricted antibiotics. *Journal of Raman Spectroscopy*, *2009*(August 2009), n/a–n/a. doi:10.1002/jrs.2505

Heywang, C., Saint-Pierre Chazalet, M., Masson, M., & Bolard, J. (1998). Orientation of anthracyclines in lipid monolayers and planar asymmetrical bilayers: a surface-enhanced resonance Raman scattering study. *Biophysical Journal*, *75*(5), 2368–2381. Retrieved from http://www.sciencedirect.com/science/article/pii/S0006349598776817

Hinterwirth, H., Kappel, S., Waitz, T., Prohaska, T., Lindner, W., & Lämmerhofer, M. (2013). Quantifying Thiol Ligand Density of Self-Assembled Monolayers on Gold Nanoparticles by Inductively Coupled Plasma–Mass Spectrometry. *ACS Nano*, *7*(2), 1129–1136. doi:10.1021/nn306024a

Hostetler, M. J., Stokes, J. J., & Murray, R. W. (1996). Infrared spectroscopy of three-dimensional self-assembled monolayers: N-alkanethiolate monolayers on gold cluster compounds. *Langmuir*, *12*(15), 3604–3612. Retrieved from http://pubs.acs.org/doi/abs/10.1021/la960249n

Hu, M., McClements, D. J., & Decker, E. A. (2003). Lipid Oxidation in Corn Oil-in-Water Emulsions Stabilized by Casein, Whey Protein Isolate, and Soy Protein

Isolate. *Journal of Agricultural and Food Chemistry*, *51*(6), 1696–1700. doi:10.1021/jf020952j

Jacobsen, C., Hartvigsen, K., Lund, P., Thomsen, M. K., Skibsted, L. H., Adler-Nissen, J., … Meyer, A. S. (2000). Oxidation in fish oil-enriched mayonnaise3. Assessment of the influence of the emulsion structure on oxidation by discriminant partial least squares regression analysis. *European Food Research and Technology*, *211*(2), 86–98. Retrieved from http://www.springerlink.com/index/BFA01KQHPUN9Q952.pdf

Jadhav, S. A. (2012). Functional self-assembled monolayers (SAMs) of organic compounds on gold nanoparticles. *Journal of Materials Chemistry*, *22*(13), 5894. doi:10.1039/c2jm14239b

Jing, C., Gu, Z., Ying, Y.-L., Li, D.-W., Zhang, L., & Long, Y.-T. (2012). Chrominance to Dimension: A Real-Time Method for Measuring the Size of Single Gold Nanoparticles. *Analytical Chemistry*, *84*(10), 4284–4291. doi:10.1021/ac203118g

Kimling, J., Maier, M., Okenve, B., Kotaidis, V., Ballot, H., & Plech, A. (2006). Turkevich Method for Gold Nanoparticle Synthesis Revisited. *The Journal of Physical Chemistry B*, *110*(32), 15700–15707. doi:10.1021/jp061667w

Kittipongpittaya, K., Chen, B., Panya, A., McClements, D. J., & Decker, E. A. (2012). Prooxidant Activity of Polar Lipid Oxidation Products in Bulk Oil and Oil-in-Water Emulsion. *Journal of the American Oil Chemists' Society*, *89*(12), 2187–2194. doi:10.1007/s11746-012-2128-5

Kneipp, K., Kneipp, H., Itzkan, I., Dasari, R. R., & Feld, M. S. (1999). Surface-enhanced Raman scattering: A new tool for biomedical spectroscopy. *Current Science*, *77*(7), 915–924.

Kong, W. H., Bae, K. H., Jo, S. D., Kim, J. S., & Park, T. G. (2011). Cationic Lipid-Coated Gold Nanoparticles as Efficient and Non-Cytotoxic Intracellular siRNA Delivery Vehicles. *Pharmaceutical Research*, *29*(2), 362–374. doi:10.1007/s11095-011-0554-y

Kyrychenko, A., Karpushina, G. V., Svechkarev, D., Kolodezny, D., Bogatyrenko, S. I., Kryshtal, A. P., & Doroshenko, A. O. (2012). Fluorescence Probing of Thiol-Functionalized Gold Nanoparticles: Is Alkylthiol Coating of a Nanoparticle as Hydrophobic as Expected? *The Journal of Physical Chemistry C*, *116*(39), 21059–21068. doi:10.1021/jp3060813

Laguerre, M., Chen, B., Lecomte, J., Villeneuve, P., McClements, D. J., & Decker, E. A. (2011). Antioxidant Properties of Chlorogenic Acid and Its Alkyl Esters in Stripped Corn Oil in Combination with Phospholipids and/or Water. *Journal of Agricultural and Food Chemistry*, *59*(18), 10361–10366. doi:10.1021/jf2026742

Larson, T. A., Joshi, P. P., & Sokolov, K. (2012). Preventing Protein Adsorption and Macrophage Uptake of Gold Nanoparticles via a Hydrophobic Shield. *ACS Nano*, *6*(10), 9182–9190. doi:10.1021/nn3035155

Lau, C. Y., Duan, H., Wang, F., He, C. Bin, Low, H. Y., & Yang, J. K. W. (2011). Enhanced Ordering in Gold Nanoparticles Self-Assembly through Excess Free Ligands. *Langmuir*, *27*(7), 3355–3360. doi:10.1021/la104786z

Li-Chan, E. C. Y. (1996). The applications of Raman spectroscopy in food science. *Trends in Food Science & Technology*, *7*(11), 361–370.

Lohbauer, U., Zipperle, M., Rischka, K., Petschelt, A., & Müller, F. a. (2008). Hydroxylation of dental zirconia surfaces: characterization and bonding potential. *Journal of Biomedical Materials Research. Part B, Applied Biomaterials*, *87*(2), 461–7. doi:10.1002/jbm.b.31126

Love, J. C., Estroff, L. A., Kriebel, J. K., Nuzzo, R. G., & Whitesides, G. M. (2005). Self-Assembled Monolayers of Thiolates on Metals as a Form of Nanotechnology. *Chemical Reviews*, *105*(4), 1103–1170. doi:10.1021/cr0300789

Ma, K., Voort, F. R., Ismail, a. a., Zhuo, H., & Cheng, B. (2000). Monitoring peroxide value in fatliquor manufacture by Fourier transform infrared spectroscopy. *Journal of the American Oil Chemists' Society*, *77*(6), 681–685. doi:10.1007/s11746-000-0109-2

McClements, D. J. (2004). *Food Emulsions: Principles, Practices, and Techniques* (Second.). CRC Press.

McCreery, R. L. (2000). *Raman Spectroscopy for Chemical Analysis* (p. 452). Wiley-Interscience.

Meurens, M., Baeten, V., Yan, S. H., Mignolet, E., & Larondelle, Y. (2005). Determination of the Conjugated Linoleic Acids in Cow's Milk Fat by Fourier Transform Raman Spectroscopy. *Journal of Agricultural and Food Chemistry*, *53*(15), 5831–5835. doi:10.1021/jf0480795

Moskovits, M. (1985). Surface-enhanced spectroscopy. *Reviews of Modern Physics*, *57*(3), 783. Retrieved from http://rmp.aps.org/abstract/RMP/v57/i3/p783_1

Muik, B., Lendl, B., Molina-Díaz, A., & Ayora-Cañada, M. J. (2005). Direct monitoring of lipid oxidation in edible oils by Fourier transform Raman spectroscopy. *Chemistry and Physics of Lipids*, *134*(2), 173–182. doi:10.1016/j.chemphyslip.2005.01.003

Muik, B., Lendl, B., Molina-Diaz, A., Valcarcel, M., & Ayora-Cañada, M. J. (2007). Two-dimensional correlation spectroscopy and multivariate curve resolution for the study of lipid oxidation in edible oils monitored by FTIR and FT-Raman spectroscopy. *Analytica Chimica Acta*, *593*(1), 54–67. doi:10.1016/j.aca.2007.04.050

Niidome, T., Yamagata, M., Okamoto, Y., Akiyama, Y., Takahashi, H., Kawano, T., … Niidome, Y. (2006). PEG-modified gold nanorods with a stealth character for in vivo applications. *Journal of Controlled Release*, *114*(3), 343–347. doi:10.1016/j.jconrel.2006.06.017

Njoki, P. N., Lim, I.-I. S., Mott, D., Park, H.-Y., Khan, B., Mishra, S., … Zhong, C.-J. (2007). Size Correlation of Optical and Spectroscopic Properties for Gold Nanoparticles. *Journal of Physical Chemistry C*, *111*(40), 14664–14669. doi:10.1021/jp074902z

Nuzzo, R. G., & Allara, D. L. (1983). Adsorption of bifunctional organic disulfides on gold surfaces. *Journal of the American Chemical Society*, *105*(13), 4481–4483. Retrieved from http://pubs.acs.org/doi/abs/10.1021/ja00351a063

Pang, S., Labuza, T. P., & He, L. (2014). Development of a single aptamer-based surface enhanced Raman scattering method for rapid detection of multiple pesticides. *The Analyst*, *139*(8), 1895–901. doi:10.1039/c3an02263c

Pieters, G., & Prins, L. J. (2012). Catalytic self-assembled monolayers on gold nanoparticles. *New Journal of Chemistry*, *36*(10), 1931. doi:10.1039/c2nj40424a

Porter, M. D., Bright, T. B., Allara, D. L., & Chidsey, C. E. (1987). Spontaneously organized molecular assemblies. 4. Structural characterization of n-alkyl thiol monolayers on gold by optical ellipsometry, infrared spectroscopy, and electrochemistry. *Journal of the American Chemical Society*, *109*(12), 3559–3568. Retrieved from http://pubs.acs.org/doi/abs/10.1021/ja00246a011

Porter, M. D., Lipert, R. J., Siperko, L. M., Wang, G., & Narayanan, R. (2008). SERS as a bioassay platform: fundamentals, design, and applications. *Chemical Society Reviews*, *37*(5), 1001–11. doi:10.1039/b708461g

Prikulis, J., Svedberg, F., Käll, M., Enger, J., Ramser, K., Goksör, M., & Hanstorp, D. (2004). Optical Spectroscopy of Single Trapped Metal Nanoparticles in Solution. *Nano Letters*, *4*(1), 115–118. doi:10.1021/nl0349606

Rana, S., Bajaj, A., Mout, R., & Rotello, V. M. (2012). Monolayer coated gold nanoparticles for delivery applications. *Advanced Drug Delivery Reviews*, *64*(2), 200–216. doi:10.1016/j.addr.2011.08.006

Rasch, M. R., Bosoy, C. A., Yu, Y., & Korgel, B. A. (2012). Chains, Sheets, and Droplets: Assemblies of Hydrophobic Gold Nanocrystals with Saturated Phosphatidylcholine Lipid and Squalene. *Langmuir*, *28*(43), 15160–15167. doi:10.1021/la302734r

Rasch, M. R., Rossinyol, E., Hueso, J. L., Goodfellow, B. W., Arbiol, J., & Korgel, B. A. (2010). Hydrophobic Gold Nanoparticle Self-Assembly with Phosphatidylcholine Lipid: Membrane-Loaded and Janus Vesicles. *Nano Letters*, *10*(9), 3733–3739. doi:10.1021/nl102387n

Rasch, M. R., Yu, Y., Bosoy, C., Goodfellow, B. W., & Korgel, B. A. (2012). Chloroform-Enhanced Incorporation of Hydrophobic Gold Nanocrystals into Dioleoylphosphatidylcholine (DOPC) Vesicle Membranes. *Langmuir*, *28*(36), 12971–12981. doi:10.1021/la302740j

Rösch, P., Popp, J., & Kiefer, W. (1999). Raman and surface enhanced Raman spectroscopic investigation on Lamiaceae plants. *Journal of Molecular Structure*, *480*, 121–124. Retrieved from http://www.sciencedirect.com/science/article/pii/S0022286098006243

Ru, E. C. Le, & Etchegoin, P. G. (2008). *Principles of surface-enhanced Raman spectroscopy and related plasmonic effects*.

Ruan, C., Wang, W., & Gu, B. (2006). Surface-enhanced Raman scattering for perchlorate detection using cystamine-modified gold nanoparticles. *Analytica Chimica Acta*, *567*(1), 114–120. doi:10.1016/j.aca.2006.01.097

Sadeghi-Jorabchi, H., Wilson, R. H., Belton, P. S., Edwards-Webb, J. D., & Coxon, D. T. (1991). Quantitative analysis of oils and fats by Fourier transform Raman spectroscopy. *Spectrochimica Acta Part A: Molecular Spectroscopy*, *47*(9–10), 1449–1458. doi:http://dx.doi.org/10.1016/0584-8539(91)80236-C

Sekiguchi, S., Niikura, K., Matsuo, Y., & Ijiro, K. (2012). Hydrophilic Gold Nanoparticles Adaptable for Hydrophobic Solvents. *Langmuir*, *28*(13), 5503–5507. doi:10.1021/la300299x

Sengupta, A., Laucks, M. L., & Davis, E. J. (2005). Surface-enhanced Raman spectroscopy of bacteria and pollen. *Applied Spectroscopy*, *59*(8), 1016–1023. Retrieved from http://www.opticsinfobase.org/abstract.cfm?id=117072

Shi, H., Zhao, G., Liu, M., Fan, L., & Cao, T. (2013). Aptamer-based colorimetric sensing of acetamiprid in soil samples: sensitivity, selectivity and mechanism. *Journal of Hazardous Materials*, *260*, 754–61. doi:10.1016/j.jhazmat.2013.06.031

Simard, J., Briggs, C., Boal, A. K., & Rotello, V. M. (2000). Formation and pH-controlled assembly of amphiphilic gold nanoparticles. *Chemical Communications*, (19), 1943–1944. doi:10.1039/b004162i

Smekal, A. (1923). Zur Quantentheorie der Dispersion. *Die Naturwissenschaften*, *11*(43), 873–875. doi:10.1007/BF01576902

Smith, E., & Dent, G. (2005). *Modern Raman Spectroscopy: A Practical Approach* (1st ed.). Wiley-Interscience.

Swami, A., Kumar, A., Selvakannan, P., Mandal, S., & Sastry, M. (2003). Langmuir–Blodgett films of laurylamine-modified hydrophobic gold nanoparticles organized at the air–water interface. *Journal of Colloid and Interface Science*, *260*(2), 367–373. doi:10.1016/S0021-9797(03)00047-X

Sweetenham, C. S., & Notingher, I. (2010). Raman spectroscopy methods for detecting and imaging supported lipid bilayers. *Spectroscopy: An International Journal*, *24*(1), 113–117. Retrieved from http://iospress.metapress.com/index/5640Q11816770UR1.pdf

Tam, N. C. M., McVeigh, P. Z., MacDonald, T. D., Farhadi, A., Wilson, B. C., & Zheng, G. (2012). Porphyrin–Lipid Stabilized Gold Nanoparticles for Surface Enhanced Raman Scattering Based Imaging. *Bioconjugate Chemistry*, *23*(9), 1726–1730. doi:10.1021/bc300214z

Tessier, P. M., Ong, K., Christesen, S. D., Lenhoff, A. M., Kaler, E. W., & Velev, O. D. (2002). Assembly of gold nanostructured films templated by colloidal crystals and use in surface-enhanced Raman spectroscopy (pp. 53–64). Retrieved from http://proceedings.spiedigitallibrary.org/proceeding.aspx?articleid=901651

Thomas, K. G., Zajicek, J., & Kamat, P. V. (2002). Surface Binding Properties of Tetraoctylammonium Bromide-Capped Gold Nanoparticles. *Langmuir*, *18*(9), 3722–3727. doi:10.1021/la015669d

Touzi, H., Chevalier, Y., Kalfat, R., Ben Ouada, H., Zarrouk, H., Chapel, J.-P., & Jaffrezic-Renault, N. (2006). Elaboration and electrical characterization of silicone-based anion-exchange materials. *Materials Science and Engineering: C*, *26*(2-3), 462–471. doi:10.1016/j.msec.2005.10.023

Tsuzuki, T., Igarashi, M., Iwata, T., Yamauchi-Sato, Y., Yamamoto, T., Ogita, K., … Miyazawa, T. (2004). Oxidation rate of conjugated linoleic acid and conjugated linolenic acid is slowed by triacylglycerol esterification and α-tocopherol. *Lipids*, *39*(5), 475–480. Retrieved from http://link.springer.com/article/10.1007/s11745-004-1253-z

Turkevich, J., Stevenson, P. C., & Hillier, J. (1951). A study of the nucleation and growth processes in the synthesis of colloidal gold. *Discussions of the Faraday Society*, *11*, 55. doi:10.1039/df9511100055

Turkevich, J., Stevenson, P. C., & Hillier, J. (1953). The formation of colloidal gold. *The Journal of Physical Chemistry*, *57*(7), 670–673. Retrieved from http://pubs.acs.org/doi/abs/10.1021/j150508a015

Waraho, T., McClements, D. J., & Decker, E. A. (2011). Mechanisms of lipid oxidation in food dispersions. *Trends in Food Science & Technology*, *22*(1), 3–13. doi:10.1016/j.tifs.2010.11.003

Weisbecker, C. S., Merritt, M. V., & Whitesides, G. M. (1996). Molecular Self-Assembly of Aliphatic Thiols on Gold Colloids. *Langmuir*, *12*(16), 3763–3772.

Weldon, M. K., Zhelyaskov, V. R., & Morris, M. D. (1998). Surface-enhanced Raman spectroscopy of lipids on silver microprobes. *Applied Spectroscopy*, *52*(2), 265–269. Retrieved from http://www.opticsinfobase.org/abstract.cfm?id=123263

Yang, H., & Irudayaraj, J. (2001). Comparison of Near-Infrared, Fourier Tansform-Infrared and Fourier Transform-Raman Methods for Determining Olive Pomace Oil Adulteration in Extra Virgin Olive Oil. *Journal of the American Oil Chemists' Society*, *78*(9), 889–895.

Yang, J., Tan, X., Shih, W.-C., & Cheng, M. M.-C. (2014). A sandwich substrate for ultrasensitive and label-free SERS spectroscopic detection of folic acid / methotrexate. *Biomedical Microdevices*. doi:10.1007/s10544-014-9871-3

Yao, W., Sun, Y., Xie, Y., Wang, S., Ji, L., Wang, H., & Qian, H. (2011). Development and evaluation of a surface-enhanced Raman scattering (SERS) method for the detection of the antioxidant butylated hydroxyanisole. *European Food Research and Technology*, *233*(5), 835–840. doi:10.1007/s00217-011-1576-8

Zhao, P., Li, N., & Astruc, D. (2013). State of the art in gold nanoparticle synthesis. *Coordination Chemistry Reviews*, *257*(3-4), 638–665. doi:10.1016/j.ccr.2012.09.002

Zhao, Y., Luo, W., Kanda, P., Cheng, H., Chen, Y., Wang, S., & Huan, S. (2013). Silver deposited polystyrene (PS) microspheres for surface-enhanced Raman spectroscopic-encoding and rapid label-free detection of melamine in milk powder. *Talanta*, *113*, 7–13. doi:10.1016/j.talanta.2013.03.075

Zheng, J., & He, L. (2014). Surface-Enhanced Raman Spectroscopy for the Chemical Analysis of Food. *Comprehensive Reviews in Food Science and Food Safety*, *13*(3), 317–328. doi:10.1111/1541-4337.12062